



# Patterns and determinants of soil CO<sub>2</sub> efflux in major forest types of Central Himalayas, India

Siddhartha Kaushal · K. S. Rao ·  
Prem Lal Uniyal · Ratul Baishya

Received: 28 January 2023 / Accepted: 6 June 2023 / Published online: 23 June 2023  
© The Author(s), under exclusive licence to Springer Nature Switzerland AG 2023

**Abstract** Soil CO<sub>2</sub> efflux ( $F_{\text{soil}}$ ) is a significant contributor of labile CO<sub>2</sub> to the atmosphere. The Himalayas, a global climate hotspot, condense several climate zones on account of their elevational gradients, thus, creating an opportunity to investigate the  $F_{\text{soil}}$  trends in different climate zones. Presently, the studies in the Indian Himalayan region are localized to a particular forest type, climate zone, or area of interest, such as seasonal variation. We used a portable infrared gas analyzer to investigate the  $F_{\text{soil}}$  rates in Himalayan tropical to alpine scrub forest along a 3100-m elevational gradient. Several study parameters such as seasons, forest types, tree species identity, age of trees, distance from tree base, elevation, climatic factors, and soil physico-chemical and enzymatic parameters were investigated to infer their impact on  $F_{\text{soil}}$  regulation. Our results indicate the warm and wet rainy season

$F_{\text{soil}}$  rates to be 3.8 times higher than the cold and relatively dry winter season. The tropical forest types showed up to 11 times higher  $F_{\text{soil}}$  rates than the alpine scrub forest. The temperate Himalayan blue pine and tropical dipterocarp sal showed significant  $F_{\text{soil}}$  rates, while the alpine *Rhododendron* shrubs the least. Temperature and moisture together regulate the rainy season  $F_{\text{soil}}$  maxima. Spatially,  $F_{\text{soil}}$  rates decreased with distance from the tree base ( $\rho = -0.301$ ;  $p < 0.0001$ ). Nepalese alder showed a significant positive increase in  $F_{\text{soil}}$  with stem girth ( $R^2 = 0.7771$ ;  $p = 0.048$ ). Species richness ( $r$ , 0.81) and diversity ( $r$ , 0.77) were significantly associated with  $F_{\text{soil}}$ , while elevation and major edaphic properties showed a negative association. Surface litter inclusion presented an elevation-modulated impact. Temperature sensitivity was exorbitantly higher in the sub-tropical pine ( $Q_{10}$ , 11.80) and the alpine scrub ( $Q_{10}$ , 9.08) forests. We conclude that the rise in atmospheric temperature and the reduction in stand density could enhance the  $F_{\text{soil}}$  rates on account of increased temperature sensitivity.

**Supplementary Information** The online version contains supplementary material available at <https://doi.org/10.1007/s10661-023-11470-9>.

S. Kaushal · K. S. Rao · P. L. Uniyal · R. Baishya (✉)  
Department of Botany, University of Delhi, Delhi 110007,  
India  
e-mail: rbaishya@botany.du.ac.in

S. Kaushal  
e-mail: kaushal.siddhartha@gmail.com

K. S. Rao  
e-mail: rao.srkottapalli@gmail.com

P. L. Uniyal  
e-mail: uniyalpl@rediffmail.com

**Keywords** Soil CO<sub>2</sub> efflux · Elevational gradient · Seasonal patterns · Spatial variation · Community structure · Temperature sensitivity

## Introduction

Soil and biotic carbon (C) pools together constitute the third largest global carbon pool, i.e., terrestrial carbon pool, with an estimated reserve of 1950–3050

petagrams (Pg) of C (Friedlingstein et al., 2020; Lal, 2008). Several other studies place the estimated reserve from 2860 to 3123 Pg C (Lal, 2008; Lal et al., 2021; Wani et al., 2022); such discrepancies are due to the uncertainties in the terrestrial carbon fluxes (Lovenduski & Bonan, 2017). The influx of carbon in terrestrial C pool is through the process of photosynthesis ( $108\text{--}120\text{ Pg year}^{-1}$ ), while the pool loses C to the atmospheric pool primarily through the process of soil respiration ( $R_s$ ) ( $60\text{--}107\text{ Pg year}^{-1}$ ) and through terrestrial fires (Hari & Tyagi, 2022; Lal, 2008). Excessive carbon emission into the atmospheric pool is critical since the labile atmospheric carbon, principally in the form of carbon dioxide, is responsible for global warming (Lashof & Ahuja, 1990). Soil respiration ( $R_s$ ) is the largest source of  $\text{CO}_2$  efflux to the atmosphere and even exceeds the  $\text{CO}_2$  release from fossil fuel combustion by seven times (Giardina et al., 2014). A slight change in  $R_s$  levels could cause significant variations in the atmospheric C pool (Trumbore, 2006). The global surface warming hiatus during 1999–2014 hints towards global temperature stabilization in the early twenty-first century. Its relapse, however, is imminent due to a rebounding increase in mean surface air temperatures (Lei et al., 2021). Estimating the levels of  $R_s$  is therefore crucial for developing climate policies.

Besides its role in the terrestrial C cycle,  $R_s$  is a prominent soil quality indicator, primarily due to its sensitivity towards vegetational changes, anthropogenic activities, soil contamination, and ecosystem degradation (Bastida et al., 2008; Cardoso et al., 2013). Soil respiration has two functional components or sources: autotrophic and heterotrophic respiration (Kuzakov, 2006), and the terms  $R_s$  and soil  $\text{CO}_2$  efflux ( $F_{\text{soil}}$ ) are erroneously used interchangeably (Maier et al., 2011). Soil respiration under instantaneous estimation is limited up to 67% through several features such as soil pore spaces, dissolution with soil water, and biological or chemical reactions (Maier et al., 2011; Sánchez-Cañete et al., 2018). Therefore, for short-term measurements, the true soil respiration rate cannot be determined, and such measurements thus give an estimate of soil  $\text{CO}_2$  efflux. The  $F_{\text{soil}}$  is a quantitative measure that describes the steady-state  $\text{CO}_2$  efflux dynamics and generally reflects the soil health (Bastida et al., 2008; Laishram et al., 2012).

Globally,  $F_{\text{soil}}$  regulation is at the temporal and spatial levels, along with perturbations from natural and

anthropogenic disturbances (Luo & Zhou, 2006). The temporal regulation of  $F_{\text{soil}}$  is primarily determined by soil temperature and moisture variations (Raich & Potter, 1995). Soil temperature influences  $F_{\text{soil}}$  by regulating microbial respiration, soil microfaunal populations, and root respiration levels, while soil moisture is regulatory only at very low (drought) or very high (waterlogging) levels (Epron et al., 1999; Fang & Moncrieff, 2001). Besides these abiotic factors, the vegetation type and substrate quality also impact  $F_{\text{soil}}$  (Jenkins & Adams, 2011). Most global and regional studies have associated temperature and moisture influences on  $R_s$  and  $F_{\text{soil}}$ , while the impact of vegetational characteristics and their spatial distribution remains largely understudied (Giardina et al., 2014; Metcalfe et al., 2011; Schurman & Thomas, 2021).

Within the terrestrial ecosystem, forests cover the most considerable portion, and trees in the forest ecosystem have the largest share of the forest C pool (Lorenz & Lal, 2010). Therefore, understanding the influence of tree species on  $F_{\text{soil}}$  could help with regional C management goals. Impact of climate change is not uniform throughout the terrestrial ecosystem. The mountain ecosystems face the most significant climate change impact (Becker & Bugmann, 2001). Climate change greatly impacts the  $R_s$  in the cold and high-latitude regions of the world (Karhu et al., 2014; Lei et al., 2021). The Himalayan mountains, especially the central and western parts, have more significant warming patterns than the average global trend (Schickhoff et al., 2016). Apart from this, the  $R_s$  and  $F_{\text{soil}}$  research in the Himalayan region remains limited, and detailed in situ studies have recently emerged using sensitive measurement techniques. Recent studies in the Himalayas focus on several aspects, viz., influence of different temperate tree species on  $R_s$  under different seasons (Kumar et al., 2023; Rawat et al., 2021); use of  $F_{\text{soil}}$  as an indicator to understand the role of a particular species (*Alnus nepalensis* D. Don) in influencing soil properties (Joshi & Garkoti, 2020); role of soil macrofauna such as termites in regulating  $F_{\text{soil}}$  (Chakraborty et al., 2021); impact of land-use systems on  $R_s$  (Bhuyan et al., 2014; Vikram et al., 2022); impact of different ecosystems on  $R_s$  (Byanjankar et al., 2020); determining the controlling factors such as temperature, precipitation, and slope aspect on  $F_{\text{soil}}$  (Dhital et al., 2022; Kumar et al., 2020); large-scale assessment of vegetational, topographic, and edaphic drivers of  $R_s$  (Pandey et al., 2023; Wangdi et al., 2017); impact of soil

erosion on terrestrial carbon loss through soil respiration (Mariappan et al., 2022); impact of forest fire on soil basal respiration (Singh et al., 2021); seasonal variation in night time  $F_{\text{soil}}$  under conifer (*Pinus roxburghii*) plantation (Singh & Parida, 2019); experimental warming impact on alpine  $R_s$  and ecosystem respiration (Tiwari et al., 2021); and even net ecosystem exchange of  $\text{CO}_2$  including  $F_{\text{soil}}$  (Singh et al., 2019).

In the IHR, older studies investigated the impact of seasons and vegetation on  $F_{\text{soil}}$  primarily using the alkali-trap-based method for  $F_{\text{soil}}$  determination (Bargali et al., 1992; Dar et al., 2015; Joshi, 1994; Ramesh et al., 2013). This method has lower sensitivity than infrared gas analyzer (IRGA)-based systems (Pongracic et al., 1997). Furthermore, studies incorporating the impact of vegetational characteristics on  $F_{\text{soil}}$  in the Himalayas are primarily restricted to specific forest type/s, species, climate zones, or land use classes (Bargali et al., 1992; Joshi, 1994; Joshi & Garkoti, 2020; Joshi et al., 1991; Kumar et al., 2023; Pandey et al., 2023; Rawat et al., 2021; Vikram et al., 2022). The elevational gradients in mountain ecosystems mimic the latitudinal patterns, and the former prove advantageous because of their steep gradients, accommodating several climate zones in smaller geographic areas. This helps to reduce the spatial extent, thus enhancing replicates for ecological studies (Sanders & Rahbek, 2012). With immense topographic heterogeneity and being climate-sensitive, Himalayan forests are key in understanding the spatio-temporal determinants and vegetational characteristics influencing soil  $\text{CO}_2$  efflux trends along wider elevational transects.

We, thus, undertook this study to understand the impact of elevation on  $F_{\text{soil}}$  in major forest types of Central Himalayas, India, covering an elevational span of 3100 m. Furthermore, we also investigated temporal, spatial, and tree species-associated features (species identity and diversity) to determine how each variable influences  $F_{\text{soil}}$  at different elevational ranges. This study is probably a first-of-its-kind study in the Indian Himalayan region (IHR) along a broader elevational gradient.

We hypothesized that (1) forest types will have different  $F_{\text{soil}}$  rates on account of the variation in species composition; (2)  $F_{\text{soil}}$  will have temporal variations (seasons) at forest type and species level due to the seasonality of soil temperature and moisture trends; (3) forest floor litter will impact total surface  $\text{CO}_2$  efflux

rates on account of litter respiration; and (4) spatial factors like distance from tree base, age class, topographic, climatic, species diversity, and edaphic factors will impact  $F_{\text{soil}}$  rates. To test these hypotheses, the primary objectives of our study included the following:

- (a) Measure  $F_{\text{soil}}$  along an elevational gradient at forest type and tree species level.
- (b) Estimate the temporal variation (seasonal) in  $F_{\text{soil}}$  rates for forest types and tree species together with the temperature sensitivity ( $Q_{10}$ ).
- (c) Measure the influence of surface litter on the  $\text{CO}_2$  efflux rates.
- (d) Calculate the impact of distance from the tree base on  $F_{\text{soil}}$  rates (spatial variation) and tree species age class (stem girth) on  $F_{\text{soil}}$  rates.
- (e) Measure the impact of elevation, species diversity, topographic, climatic, soil physical, chemical, and enzymatic properties on  $F_{\text{soil}}$  rates.

## Materials and methods

### Study area description

Nine forest stands were selected in the Garhwal region of Uttarakhand, India (Fig. 1). Uttarakhand represents the Indian portion of the Central Himalayas, referred to as the Indian Central Himalayas (ICH). The ICH has 44 recognized forest types (Champion & Seth, 1968). Based on site accessibility and protected area status (to reduce anthropogenic interference), nine forest stands were selected representing nine forest types (FT) (Table 1, Fig. 1). Forest types selected are major forest types, as they represent 63.42% of the total forest cover of the state (FSI, 2019). The study sites lie between the geographic bounds of  $30^\circ 00'$  to  $30^\circ 46'$  N latitude and  $77^\circ 48'$  to  $79^\circ 13'$  E longitude (Fig. 1), covering a wide elevational span from 360 to 3510 m (Table 1).

The forest type FT1 lie in the core zone of Rajaji National Park. Forest types FT2, FT4, and FT6 are reserve forests, while FT3, FT5, FT7, FT8, and FT9 lie in the core zone of the Kedarnath Wildlife Sanctuary. The climate of the study area has three distinct seasons: cold and relatively dry winter season (November–February), warm and dry summer season (April–June), and warm and wet rainy season (July–September). Short

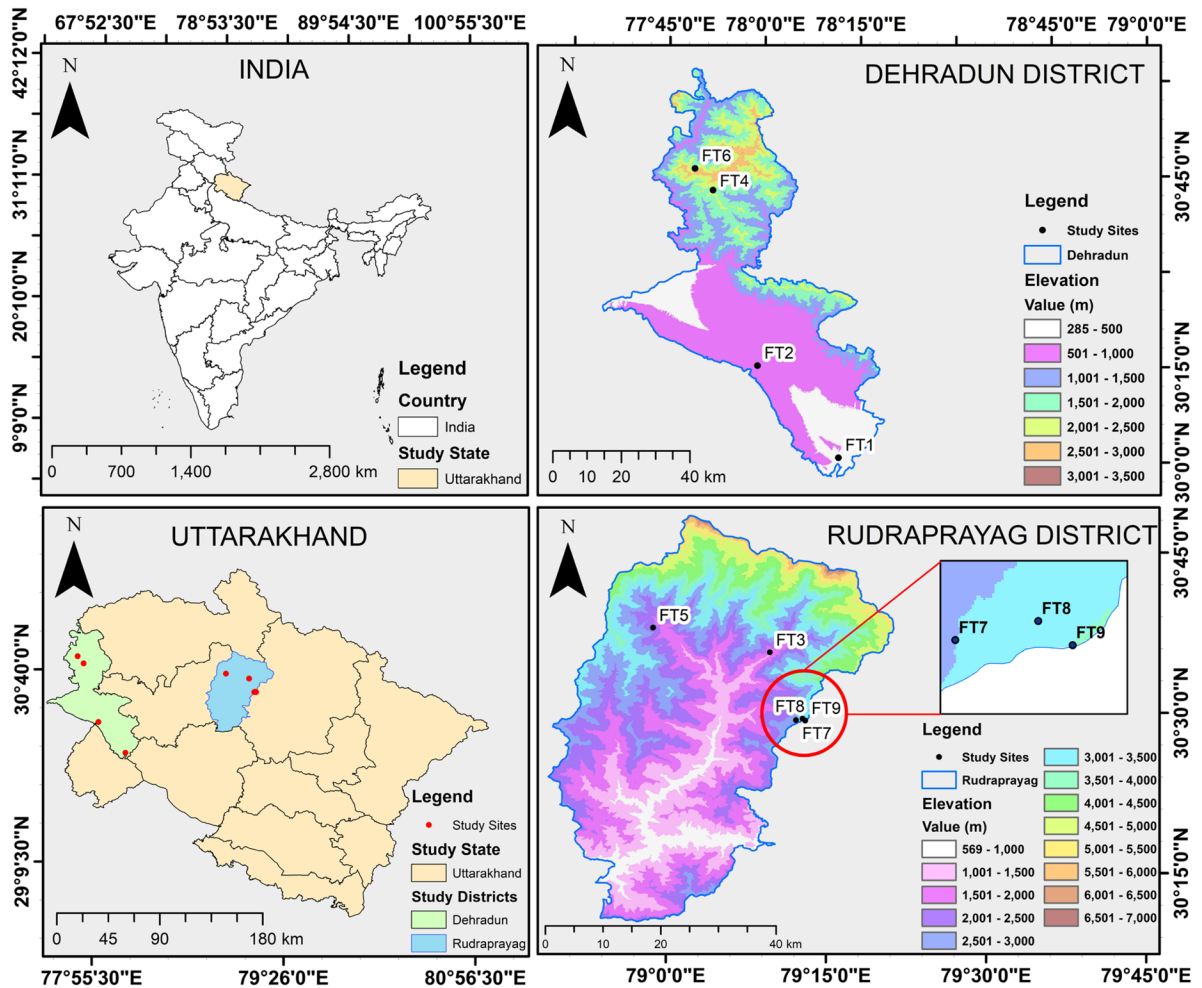


**Fig. 1** Study area map. Map of India showing study state Uttarakhand, map of Uttarakhand showing study districts with sites, and the elevational gradient map of districts Dehradun

and Rudraprayag showing the nine study sites. FT1 to FT9 refer to forest types 1 to 9, respectively

spring and autumn seasons are prevalent during March and October, respectively (Singh & Singh, 1987). The winter season in the sub-alpine to alpine regions may extend up to April (Rai et al., 2012). The forest types FT3–FT9 receive snowfall during the winter months, with FT5–FT9 receiving heavy snowfall, leading to high snow density and depth. Therefore, we collected the  $F_{\text{soil}}$  measurements in these forest stands either after the first spell of light snowfall or during the first week of December, when the precipitation chances are lower (Fick & Hijmans, 2017). Overall, the study area experiences a monsoon climate with maximum rainfall during July and August and the least from October to December. Within the study area's elevational range (Table 1),

the average maximum monthly temperature ranged from 17.19 to 38.23 °C, while the average minimum monthly temperature ranged from –5.44 to 6.97 °C (Fick & Hijmans, 2017).

The vegetational characteristics, community structure, and anthropogenic disturbance levels for each forest type (except FT9) have been detailed previously (Kaushal et al., 2021). The dwarf *Rhododendron* scrub forest (FT9) at Chandrashila is dominated by an alpine shrub species, *Rhododendron anthopogon* D.Don (Rai et al., 2012).

Along the elevational gradient, the forest types lie in the Cenozoic Himalayan Foreland Basin, Inner Lesser Himalayan sedimentary belt, and Higher Himalayan

**Table 1** Vegetational and topographic characteristics of studied forest types

Forest type (FT) code	Location (district)	Dominant tree species <sup>a</sup>	Forest type <sup>b</sup>	Elevation (m.a.s.l.)	Slope <sup>c</sup> (slope aspect)	Max Temp. <sup>d</sup> (°C)	Min Temp. <sup>e</sup> (°C)	Rainfall <sup>f</sup> (mm)
FT1	Motichur Range (Dehradun)	<i>Shorea robusta</i> C.F.Gaertn	Moist Shiwalik sal forest (3C/C <sub>2</sub> a)	360	3.01 (W)	29.48	17.10	1528
FT2	Asarori Range (Dehradun)	<i>Shorea robusta</i>	Bhabar-Dun sal forest (3C/C <sub>2</sub> b(i))	692	3.63 (NW)	27.35	15.52	1983
FT3	Gondar (Rudraprayag)	<i>Pinus roxburghii</i> Sarg	Himalayan chir pine forest (9/C <sub>1</sub> b)	1710	30.84 (E)	20.22	9.40	1361
FT4	Chakrata Range (Dehradun)	<i>Quercus leucotrichophora</i> A.Camus	Ban oak forest (12/C <sub>1</sub> a)	2109	36.21 (E)	19.14	9.63	1734
FT5	Triyuginarayan (Rudraprayag)	<i>Neolitsea pallens</i> (D.Don) Momiy. & H.Hara	Moist temperate deciduous forest (12/C <sub>1</sub> e)	2210	20.48 (NE)	17.80	8.02	1631
FT6	Kanasar Range (Dehradun)	<i>Cedrus deodara</i> (Roxb. Ex D.Don) G.Don	Moist deodar forest (12/C <sub>1</sub> c)	2342	27.87 (W)	17.86	9.03	1624
FT7	Chopta (Rudraprayag)	<i>Rhododendron arboreum</i> Sm	Kharsu oak forest (12/C <sub>2</sub> a)	2981	29.75 (W)	12.94	3.89	2028
FT8	Tungnath (Rudraprayag)	<i>Abies spectabilis</i> (D.Don) Mirb	West Himalayan sub-alpine high-level fir forest (14/C <sub>1</sub> a)	3296	19.62 (NW)	11.81	2.81	1982
FT9	Chandrashila (Rudraprayag)	Alpine meadow	Dwarf <i>Rhododendron</i> scrub (15/E <sub>1</sub> )	3510	19.94 (NW)	11.16	2.17	1931

The climate data is sourced from WorldClim (Ver. 2.1) and represents the data average from 1970 to 2000

<sup>a</sup>The data for dominant tree species were obtained from Kaushal et al. (2021)

<sup>b</sup>The forest-type classification is based on Champion and Seth (1968). Values in parentheses indicate the forest-type code as per the forest-type classification of India

<sup>c</sup>Slope is represented in degrees. For the slope aspect, *W* west direction, *NW* northwest direction, *E* east direction, *NE* northeast direction

<sup>d,e</sup>Average annual maximum and minimum temperature

<sup>f</sup>Total annual rainfall

Crystallines belt. The major geologic constituents in the study sites are sandstones, shales, carbonates, mica schists, gneisses, and granites (Jain, 2020). Based on the digital FAO-UNESCO soil map of the world (FAO, 2007), the tropical forest types FT1 and FT2 have

Calcaric Fluvisols soil types. Dystric Cambisols make up the FT4 and FT6 soil types, whereas Lithosols, Humic Cambisols, and Rankers combine to form the primary soil type for FT3, FT5, FT7, FT8, and FT9, respectively (Supplementary Fig. S1).

## Study sampling design and acquisition of remotely sensed topographic and climate data

A preliminary reconnaissance survey for the analyses of  $F_{\text{soil}}$  was carried out from September to December 2020. The standard quadrat method was used for vegetation sampling and  $F_{\text{soil}}$  measurements. In FT1 to FT6, ten square quadrats of dimension 1000 m<sup>2</sup> (31.6 m × 31.6 m) were randomly laid in each forest type to cover 1 ha of area (Kaushal & Baishya, 2021; Kaushal et al., 2021). In FT7 and FT8, due to undulating terrain and unpredictable weather conditions, five quadrats (1000 m<sup>2</sup>) were laid in each forest type. In alpine forest type FT9, five quadrats of 25 m<sup>2</sup> (5 m × 5 m) were laid due to the limited terrain and being a tapering mountain peak (Chandrashila Peak). Therefore, the total area surveyed in this study for the in situ  $F_{\text{soil}}$  measurements was 7.0125 ha. All the  $F_{\text{soil}}$  measurements were conducted within the permanent plots established.

Site-specific topographic estimates of elevation, slope, and slope aspects were classified from the digital elevation model (DEM) data of the shuttle radar topography mission (SRTM) at 1-Arcsec spatial resolution (ca. 26 m at 30° latitude) (<https://earthexplorer.usgs.gov/>). The average monthly climate data, viz., minimum temperature ( $T_{\text{min}}$ ) (°C), maximum temperature ( $T_{\text{max}}$ ) (°C), precipitation (mm), solar radiation (kJ m<sup>-2</sup> day<sup>-1</sup>), and water vapor pressure (kPa), was extracted from WorldClim global dataset at 30-Arcsec resolution (Ver. 2.1 released, 2020) (Fick & Hijmans, 2017). The topographic and climate raster layers were processed using ArcGIS (ver. 10.5) software.

## Determination of in situ soil CO<sub>2</sub> efflux ( $F_{\text{soil}}$ )

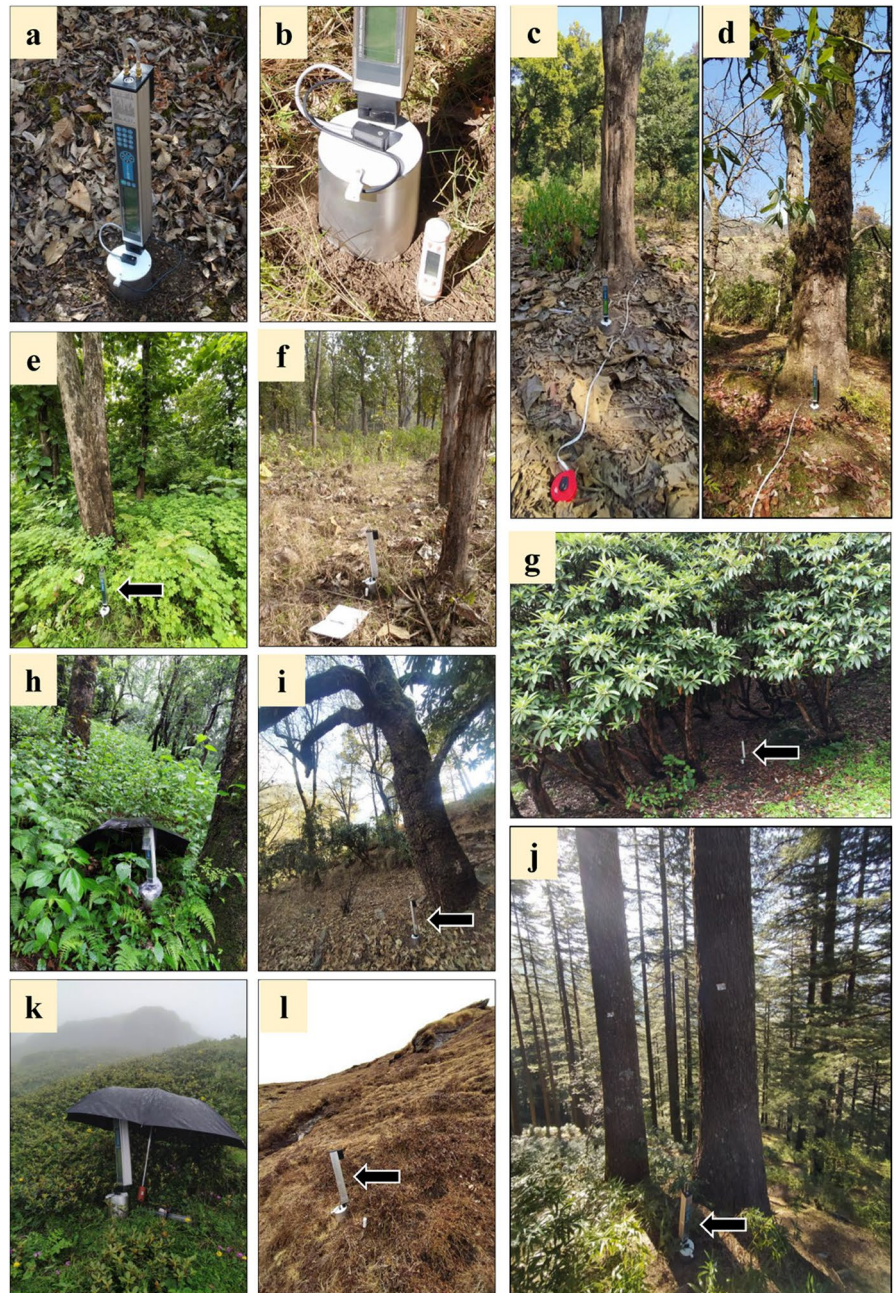
The in situ  $F_{\text{soil}}$  was measured from February 2021 to June 2022 using the CI-340 Portable Photosynthesis System (CID Bio-Science, Inc., USA) (Fig. 2a) equipped with a CI-301SR soil respiration chamber (Fig. 2b). The chamber has an area of 73.4 cm<sup>2</sup> and a volume of 0.58 liters when inserted to a depth of 1 cm in the soil. CI-340 is an environmentally sealed, non-dispersive infrared gas analyzer (IRGA) unit coupled with a gas pump, flow regulators, and environmental analyzers. The system was operated in closed-system

mode with 1-s sampling (IRGA detection) interval, 0.5–1 min<sup>-1</sup> gas flow rate, and 15 to 180 s of measurement time. The measurement time varied to accommodate the  $F_{\text{soil}}$  range since a shorter sampling time (15 s) avoids the oversaturation of the analyzer (2200 ppm CO<sub>2</sub>) during measurement. An infrared (IR) temperature sensor attached to the soil chamber determines the soil surface ( $T_0$ ) temperature (°C), while a photosynthetically active radiation (PAR) sensor determines the incoming PAR values (μmol m<sup>-2</sup> s<sup>-1</sup>) (Fig. 2b).

The  $F_{\text{soil}}$  in the studied forest types was randomly analyzed at two points within each quadrat. Thus, for the 75 quadrats laid in the study, 150  $F_{\text{soil}}$  measurements were taken which represents 20  $F_{\text{soil}}$  measurements each for FT1–FT6 and 10 each for FT7–FT9 for a particular season. The measurements were taken at least 3–5 m from any tree or large shrub to avoid the undue effects of specific plant species. Before inserting the chamber, freshly fallen and surface litter was removed, and any herbaceous growth was clipped with field scissors to avoid CO<sub>2</sub> capture due to photosynthesis (Fig. 2a and g). Forest type-specific  $F_{\text{soil}}$  estimates were collected seasonally to determine the temporal (seasonal) influence. The  $F_{\text{soil}}$  under forest types and dominant or major tree species (Fig. 2j) was measured separately in two seasons, i.e., rainy and winter (Fig. 2e, f, h, i, k, and l). These seasons were selected due to the maximum differential in their temperature and precipitation parameters. The summer season (May–June) and the rainy season were alike in terms of temperature parameters. It was thus not included and only used for exploratory measurements in climax forest types, viz., FT1, FT3, FT4, and FT6. For tree species-specific  $F_{\text{soil}}$  measurements, around 15–20 replicates were collected per species per season and these measurements are independent of the seasonal forest-type  $F_{\text{soil}}$  determination. The measurements were made during the peak period of the winter (December–January) and rainy season (July–August). Only one set of measurements was taken for each season to reduce the within-season variability.

Organic litter-associated CO<sub>2</sub> efflux was estimated by placing the chamber on the ground without removing the surface litter, followed by a second measurement after clearing the surface litter. For the impact of litter on  $F_{\text{soil}}$ , we randomly sampled 15 replicates within the permanent quadrats for each forest type.

**Fig. 2** Quantification of in situ  $F_{soil}$  rates. **a** CI-340 Portable IRGA with CI-301SR soil chamber in closed-system mode (see the looped connector tube on the top); **b** soil chamber with IR temperature sensor and PAR sensor; also notice a soil temperature probe inserted next to the chamber; distance effect from tree base under **c** *Tectona grandis* (FT1) and **d** *Aesculus indica* (FT5); temporal effect under rainy and winter season respectively at FT1 (**e, f**), FT3 (**h, i**), and FT9 (**k, l**); notice the effect of season on the ground flora; **g**  $F_{soil}$  under forest type (note equidistant placement) at FT7; **j**  $F_{soil}$  determination under tree species base (*Cedrus deodara*, FT6)



The effect of distance from the tree base (spatial variation) on  $F_{soil}$  was determined for dominant or major tree species (Kaushal et al., 2021) at three distances from the tree base, viz., 0 cm (just under the tree trunk), 100 cm, and 250 cm (Fig. 2c, d). Around 5–10 individuals of each tree species were randomly selected for the distance effect. The influence of age

class (determined using stem girth) on  $F_{soil}$  was estimated at the base of dominant or major tree species under varying stem girths. The forest types studied had individuals of various girth classes (Kaushal & Baishya, 2021), and around 10–20 individuals were selected for each species, incorporating the maximum girth range available.

## Quantification of soil physical, chemical, and enzymatic properties

Samples for soil analyses (FT1 to FT8 only; FT9 excluded owing to rugged terrain) were randomly collected from two points within each quadrat during the rainy and winter seasons (70 quadrats  $\times$  2 samples per quadrat  $\times$  2 seasons). Soil samples were collected from 0 to 10 cm soil depth using a soil hoe by excavating a 10 cm  $\times$  10 cm  $\times$  10 cm soil block. We selected the 0 to 10 cm soil depth since this layer contains the maximum amount of organic matter undergoing decomposition, the presence of surface litter with associated microbial faction, litter leachates, and the maximum contribution of nutrients from throughfall and stemflow. This soil layer is also directly in contact with the atmospheric temperature, moisture conditions, and plant roots. All replicate samples for a forest type were homogenized and reduced using the quartering method. Soil samples were sieved using a 2-mm sieve prior to soil analyses. Soil temperature was measured up to a depth of 0–15 cm ( $T_{15}$ ) using a soil probe thermometer (R-tek<sup>®</sup> digital thermometer) (Fig. 2b). Soil moisture was determined gravimetrically at 105 °C in a forced hot-air oven and expressed as a percentage of dry soil weight (Anderson & Ingram, 1993). Soil pH<sub>H2O</sub> was determined using field moist 2-mm sieved soil in a 1:2.5 (w/v) ratio of soil and de-ionized water solution (Anderson & Ingram, 1993). Soil electrical conductivity was determined in a 1:2 (w/v) solution of fresh sieved soil and de-ionized water using a handheld conductivity tester (PCSTestr<sup>™</sup> 35, Eutech Instruments). Soil organic carbon (SOC) was determined in sieved air-dried finely ground soil samples using IRGA-based elemental analyzer (liquiTOC II, Elementar GmbH, Germany). Total Kjeldahl nitrogen (TKN) was determined by Kjeldahl digestion and steam distillation using an automatic distillation unit (UDK149, VELP Scientifica, Italy). Soil available phosphorous was determined using 2.5% acetic acid extraction and molybdenum blue chemistry (Allen et al., 1974). Soil exchangeable potassium was estimated using 1 M neutral ammonium acetate extraction and subsequent determination using flame photometry (Flame Photometer 128, Systronics, Ahmedabad). Soil dehydrogenase enzyme activity (DHA) was determined in fresh sieved soil by 2, 3, 5-triphenyltetrazolium chloride (TTC) reduction assay (Casida, 1977).

The effect of temperature dependence (temperature sensitivity— $Q_{10}$ ) on  $F_{\text{soil}}$  was determined using the  $Q_{10}$  coefficient (Mundim et al., 2020) at the forest-type level and for individual tree species. The  $Q_{10}$  value was calculated using a first-order exponential equation (Eq. 1) (Fang & Moncrieff, 2001):

$$Q_{10} = \left( \frac{R_2}{R_1} \right)^{10/(T_2 - T_1)} \quad (1)$$

Here,  $Q_{10}$  is the temperature sensitivity factor;  $R_1$  and  $R_2$  refer to  $F_{\text{soil}}$  rates under two seasons with temperatures (in °C)  $T_1$  and  $T_2$ , respectively, with consideration of  $T_2 > T_1$ . The average of  $F_{\text{soil}}$  rates for a particular season and soil temperature (0–15 cm depth) were used for  $Q_{10}$  measurements.

## Statistical analyses

The data were first tested for the assumption of normality using Shapiro–Wilk’s test and for homoscedasticity using Levene’s test. An Independent sample *t*-test was conducted to determine the significant difference between the means for the rainy and winter seasons among each forest type and tree species-specific  $F_{\text{soil}}$  measurements. Welch’s one-way analysis of variance (ANOVA) with the Games-Howell post hoc test was used to test significant differences between the  $F_{\text{soil}}$  means (for different forest types of a particular season) and the comparison of summer, rainy, and winter season  $F_{\text{soil}}$  rates for the forest types. Parametric ANOVA with Tukey’s HSD post hoc test was used to determine the significant difference in assessing spatial variation, i.e., distance from tree base effect on  $F_{\text{soil}}$  rates. A paired-sample *t*-test was used to assess the impact of surface litter on  $F_{\text{soil}}$  rates. Linear and non-linear regressions were performed to determine the relationship between the tree stem girth (independent variable) and  $F_{\text{soil}}$  rate (dependent variable) for different tree species under different forest types.

A two-tailed Pearson correlation analysis was used to determine the degree and direction of association between the  $F_{\text{soil}}$  rates (under rainy and winter seasons); topographic, climatic, and tree species diversity (Kaushal et al., 2021); tree species biomass stock (Kaushal & Baishya, 2021); and soil properties. A factor reduction analysis as principal component analysis (PCA) was performed with forest-type  $F_{\text{soil}}$  rates, climatic, topographic, species diversity, biomass, and



soil properties. The PCA was performed using a correlation matrix. Components with Eigenvalues > 1 were retained as principal components (Kaiser’s rule) (Zuur et al., 2007). The PCA loading correlations and biplot were used to interpret the factor reduction results.

All statistical analyses were conducted at a 5% significance level either using SPSS ver. 23 (IBM, USA) or PAST ver. 4.11 software (Hammer et al., 2001). The graphs were plotted using GraphPad Prism ver. 9.5.0 for Windows (GraphPad Software, USA).

### Results

In this investigation, ca. 1200  $F_{soil}$  measurements were recorded and further scrutinized to exclude erroneous observations due to inaccurate measurements, improper gas flow rate, and poor soil chamber fit.

$F_{soil}$  rates under different forest types and seasons (temporal effect)

Among all forest types, FT1 had the highest  $F_{soil}$  rate ( $10.37 \mu\text{mol m}^{-2} \text{s}^{-1}$ ) during the rainy season and FT5 ( $4.42 \mu\text{mol m}^{-2} \text{s}^{-1}$ ) during the winter (Fig. 3). The FT9 had the least  $F_{soil}$  value among all the forest types for both the seasons. All forest types showed a statistically significant difference between the means of  $F_{soil}$  for rainy and winter seasons (Fig. 3 and Supplementary Table S1). Throughout the forest types, the rainy season had an average of 3.8 times higher  $F_{soil}$  rates than the winter, with the increment level ranging from 1.8 (FT5) to 11.5 (FT9) times. The forest types showed a statistically significant difference in  $F_{soil}$  rates during the rainy (Welch’s  $F(8, 28.3)$ ,  $11.22$ ;  $p < 0.0001$ ) and the winter season (Welch’s  $F(8, 19.4)$ ,  $36.08$ ;  $p < 0.0001$ ). However, the Games-Howell post hoc test showed the non-significance of  $F_{soil}$  rates between several forest types for a particular season (Supplementary Table S1). FT5 and FT9 showed the least spread in the  $F_{soil}$  rates for the rainy and winter seasons, respectively, with a smaller interquartile range (Fig. 3).

A significant difference was observed between the summer, rainy, and winter seasons’  $F_{soil}$  rates (Fig. 4 and Supplementary Table S2). The Games-Howell post hoc test showed that the tropical (FT2) and sub-tropical (FT3) forest types significantly differ for the rainy season  $F_{soil}$  values from the other two seasons.

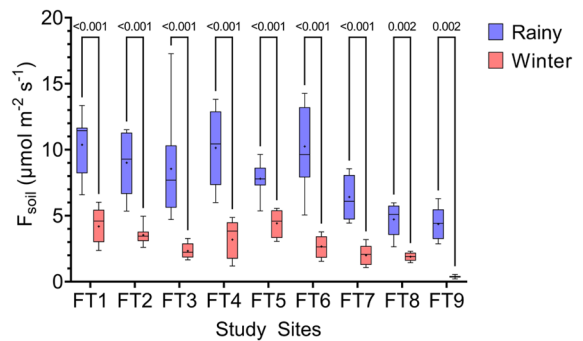


**Fig. 3** Box-whisker plot representing the soil CO<sub>2</sub> efflux rates for forest types studied under two seasons. The boxes extend from the 25<sup>th</sup> to 75<sup>th</sup> percentile with the median represented by a bar and the mean by the plus sign. The whiskers represent the smallest and the largest data value

However, the summer and winter seasons’  $F_{soil}$  did not differ significantly. This trend was not consistent for the temperate (FT4 and FT6) forest types, where all three seasons varied significantly (Fig. 4). Nonetheless, all the forest types had the rainy season with the highest  $F_{soil}$  rate.

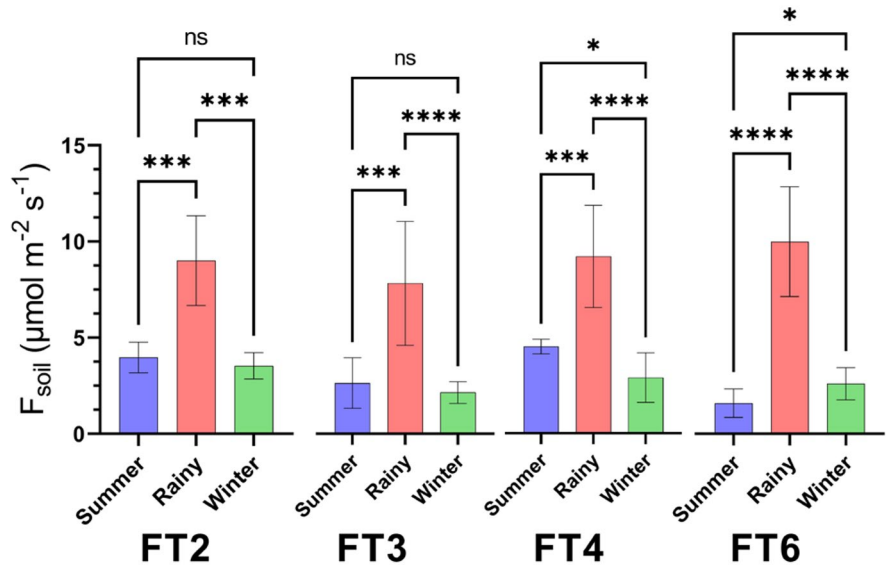
The  $Q_{10}$  values for the forest type ranged from 1.6 (FT5) to 11.8 (FT3), with the average  $Q_{10}$  value being 4.09. The sub-tropical pine (FT3:  $Q_{10}$  11.8) and alpine scrub (FT9:  $Q_{10}$  9.08) forest types had exceptionally high-temperature sensitivity, while all the remaining forest types ranged between 1.60 and 2.67 (Supplementary Table S1).

$F_{soil}$  rates under dominant/major tree species in different forest types and seasons

Temperate *Pinus wallichiana* A.B.Jacks. ( $12.6 \mu\text{mol m}^{-2} \text{s}^{-1}$ ) and tropical *S. robusta* ( $4.47 \mu\text{mol m}^{-2} \text{s}^{-1}$ ) had the highest  $F_{soil}$  rates among tree species in rainy and winter seasons, respectively (Supplementary Table S3, Fig. 5). Alpine dwarf shrub *R. anthopogon* had the least  $F_{soil}$  rate for both the seasons among the species (Fig. 5).

Almost all the tree species investigated showed a significant difference in the means for both seasons in the  $F_{soil}$  rates (Fig. 5). The highest  $F_{soil}$  increment from winter to rainy season was 548% in *R. anthopogon* (FT9), followed by 328% in *Rhododendron arboreum* (FT3), and 320% in *P. wallichiana* (FT6). The average increment for all the species taken together was 190%.

**Fig. 4** Comparison of summer season soil CO<sub>2</sub> efflux rates for rainy and winter seasons. Bars represent the mean while the error bars represent the standard deviation. \**p* < 0.05, \*\*\**p* < 0.001, \*\*\*\**p* < 0.0001, and ns: *p* > 0.05



This research recorded the highest *Q*<sub>10</sub> value for tree species in the sub-tropical pine forest (Supplementary Table S3) viz., *R. arboreum* (12.25) > *P.*

*roxburghii* (11.94) > *Alnus nepalensis* (6.11). Interestingly, *R. arboreum* showed the highest (FT3, *Q*<sub>10</sub> 12.25) and lowest (FT5, *Q*<sub>10</sub> 1.77) temperature

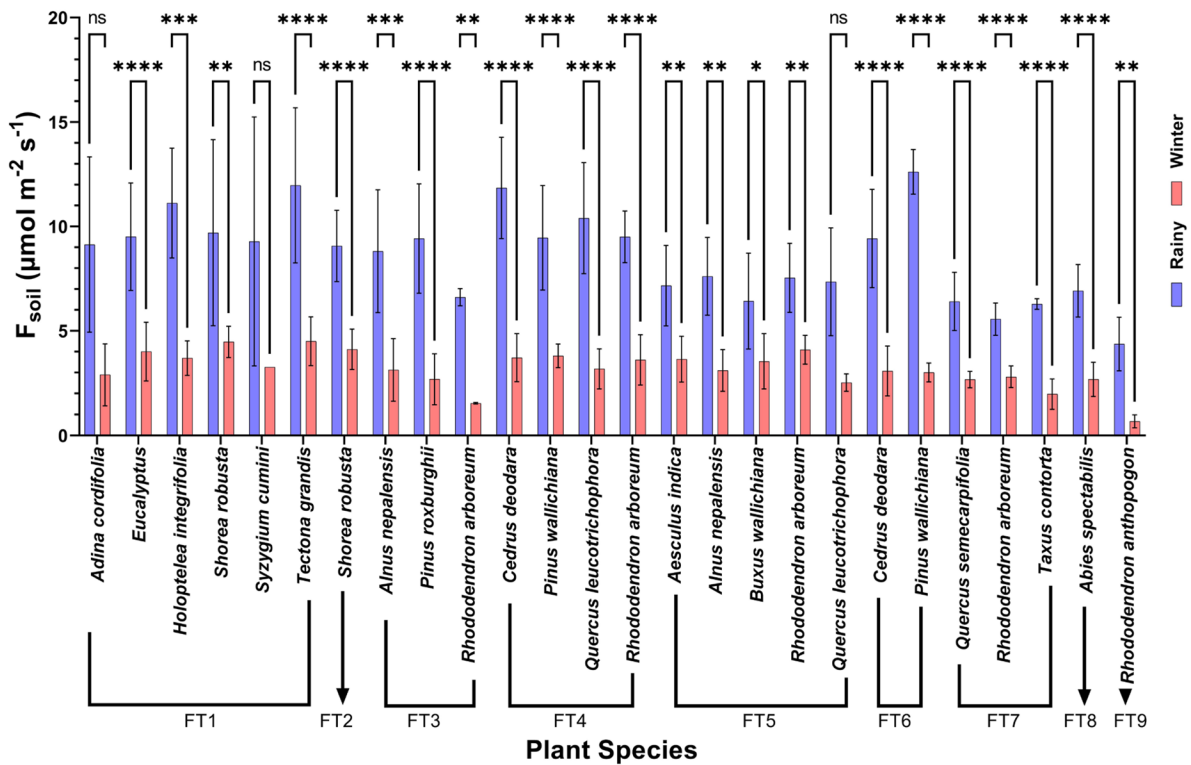


**Fig. 5** Soil CO<sub>2</sub> efflux rates for dominant/major tree species under rainy and winter seasons among different forest types along an elevational gradient. Bars represent the mean, while the

error bars represent the standard deviation. \**p* < 0.05, \*\**p* < 0.01, \*\*\**p* < 0.001, \*\*\*\**p* < 0.0001, and ns: *p* > 0.05

sensitivity values in different forest types under different elevations.

Impact of surface litter on  $F_{soil}$  and distance from tree base (spatial variation)

The  $F_{soil}$  measurements with surface litter yielded discordant results among the forest types (Fig. 6, Supplementary Table S4). Irrespective of statistical significance, only the tropical (FT1) and sub-tropical (FT3) forest types showed higher  $F_{soil}$  rates (around 1.2 times higher) with surface litter. In contrast, the temperate sites (FT4, FT5, FT6, and FT7) showed the opposite. Statistically, FT3, FT4, and FT7 showed no significant differences in  $F_{soil}$  rates with and without surface litter as determined through paired sample *t*-tests (Fig. 6).

Only two tree species, i.e., *T. grandis* (FT1) (Fig. 7a) and *Aesculus indica* (FT5) (Fig. 7b), showed a statistically significant difference between the distances for  $F_{soil}$  rates. Generally, most species'  $F_{soil}$  rate was the highest closest to the tree base (Supplementary Table S5). The average  $F_{soil}$  for all the species combined (Fig. 7c) in terms of spatial variation showed a significant difference ( $F(2, 36): 9.299; p=0.0006$ ). The average  $F_{soil}$  rate near the tree base (0 cm) was 1.24 and 1.31 times greater than the  $F_{soil}$  rates at 100 and 250 cm distances from the tree base. Non-parametric Spearman's correlation between the distance from tree base and  $F_{soil}$  rates showed a weak negative statistically significant correlation ( $\rho = -0.301; p < 0.0001$ ) (Fig. 7d).

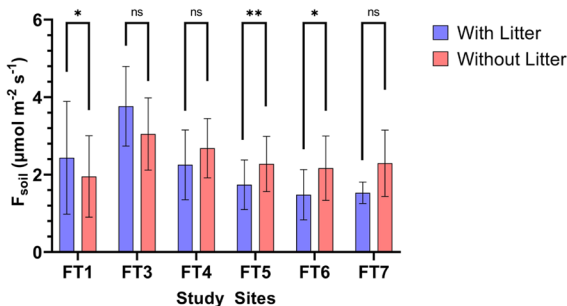


**Fig. 6** Effect of the inclusion of surface litter on soil CO<sub>2</sub> efflux rates. Bars represent the mean, while the error bars represent the standard deviation. \**p* < 0.05, \*\**p* < 0.01, and ns: *p* > 0.05

Effect of tree age (stem girth) and elevation on tree species  $F_{soil}$  rates

We tested one dominant/major tree species from the 8 tree-bearing forest types (FT1–FT8) for the impact of stem girth on  $F_{soil}$  rates using linear and non-linear regression models. Only *A. nepalensis* (FT5) showed a significant positive linear effect ( $R^2=0.7771; p=0.048$ ) on  $F_{soil}$  ( $2.25\text{--}4.58 \mu\text{mol m}^{-2} \text{s}^{-1}$ ) with increase in tree stem girth (103–300 cm) (Fig. 8).

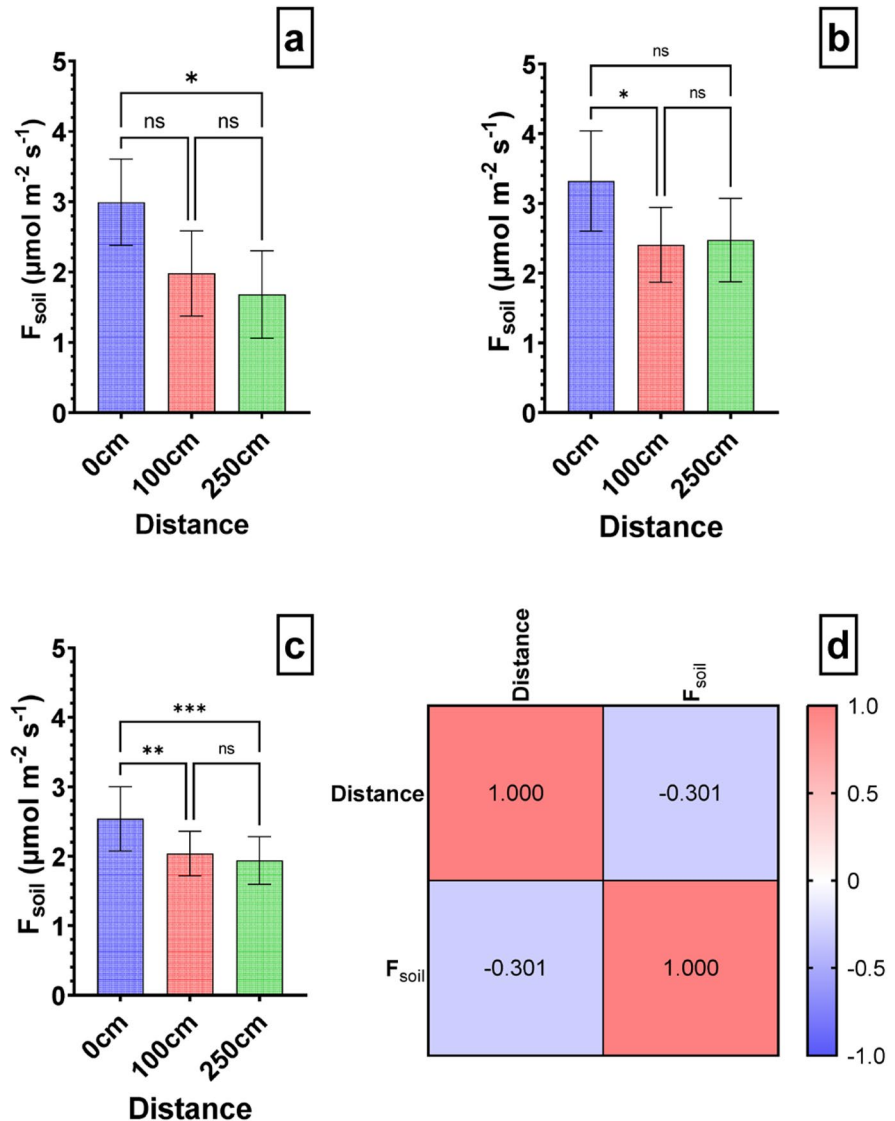
To observe the impact of elevation on  $F_{soil}$ , we selected *R. arboreum* due to its widest occurrence range (1710 m at FT3 to 2981 m at FT7). Under both seasons, the species showed a difference in  $F_{soil}$  rates at different elevations (Fig. 9) (Rainy season:  $F(3, 18), 14.087; p < 0.0001$  and winter season: Welch's  $F(3, 7.5), 33.120; p = 0.004$ ). The post hoc tests showed *R. arboreum* to have the highest  $F_{soil}$  rate in mid-temperate elevations, i.e., FT4 (2109 m) and FT5 (2210 m) under rainy and winter seasons, respectively (Fig. 9).

Statistical data analyses

The  $F_{soil}$  rates for both seasons positively correlated with the average annual maximum and minimum air temperature, water vapor pressure, and atmospheric pressure. The  $F_{soil}$  showed a strong negative correlation with elevation (Supplementary Fig. S4). Interestingly, all the positively correlating variables mentioned above showed a strong negative correlation with elevation. Annual average precipitation, solar radiation, PAR, slope, and slope aspect did not show a significant association with  $F_{soil}$  for either season (Supplementary Fig. S4).

The  $F_{soil}$  for the rainy season did not significantly correlate with tree species diversity, richness, and biomass parameters. In contrast, the  $F_{soil}$  for the winter season showed a moderate to strong positive correlation with species richness ( $r=0.81, p=0.015$ ) and species diversity ( $r=0.77, p=0.024$ ) (Supplementary Figure S2). Furthermore, the winter season  $F_{soil}$  rates did not correlate with any soil parameter. In contrast, the rainy season  $F_{soil}$  rate showed a strong negative correlation with soil moisture ( $r=-0.85, p=0.007$ ), SOC ( $r=-0.73, p=0.039$ ), TKN ( $r=-0.76, p=0.029$ ), and DHA activity ( $r=-0.75, p=0.03$ ). The soil pH positively correlated with the rainy season  $F_{soil}$  rate ( $r=0.78, p=0.023$ ) (Supplementary Figure S3).

**Fig. 7** Impact of distance from the tree base on soil CO<sub>2</sub> efflux rates. **a** for *Tectona grandis* (FT1), **b** for *Aesculus indica* (FT5), **c** average for all the species combined, and **d** Spearman's correlation between  $F_{soil}$  rates and distance from the tree base. Bars represent the mean, while the error bars represent the standard deviation. \* $p < 0.05$ , \*\* $p < 0.01$ , \*\*\* $p < 0.001$ , and ns:  $p > 0.05$



The dimension reduction PCA for both seasons had the first four principal components (PCs) with eigenvalues > 1. The first four PCs explained 91.12% and 89.37% of the total variance for rainy and winter season data, respectively (Supplementary Table S6). The PCA biplot (Fig. 10) is illustrated for PC1 and PC2 since these two PCs explained the highest variance under both seasons.

PCA biplot for both seasons (Fig. 10) indicated a clear ordination of sites along PC1. The tropical and sub-tropical forests were in the positive space of PC1, while the temperate–alpine forest types in the negative space. For PC2, the forest types FT1, FT4,

FT5, FT6, and FT7 were present in the positive space for the rainy season, while only FT1, FT5, and FT6 were for the winter season. A three-dimensional (3D) representation of the site score plot (Supplementary Fig. S5) under both seasons and the loading correlations (Supplementary Table S7) was used to visualize the ordination of sites on the principal axes.

During the rainy season, soil temperature, atmospheric temperature variables, water vapor pressure, and atmospheric pressure positively influence the variable loadings on PC1. In contrast, elevation and soil properties show a negative influence. This trend is also similar in the winter season. The PC2,

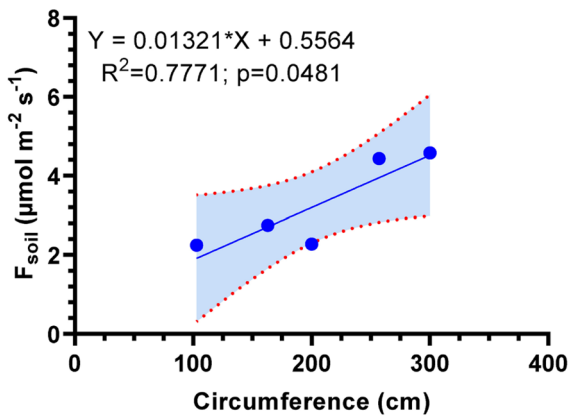


**Fig. 8** Simple linear regression between the tree’s circumference and the corresponding  $F_{soil}$  rate for *Alnus nepalensis* (site 5). The regression line is indicated in blue, the observations are indicated by blue dots, the red-dotted lines mark the extent of the confidence interval (95%), and the area under it is in a blue shade

however, had different trends in both seasons. In the rainy season, precipitation, soil electrical conductivity (EC), and total biomass density (TBD) were major influencing variables. In the winter season, the influencing variables were primarily tree species richness, species diversity, TBD, and EC. The 3D scatter plot (Supplementary Fig. S5) also indicates that FT1 and FT2 ordinate on the right corners, while FT7 and FT8 are on the left. The remaining sites were grouped roughly in the center of the PCA plot.

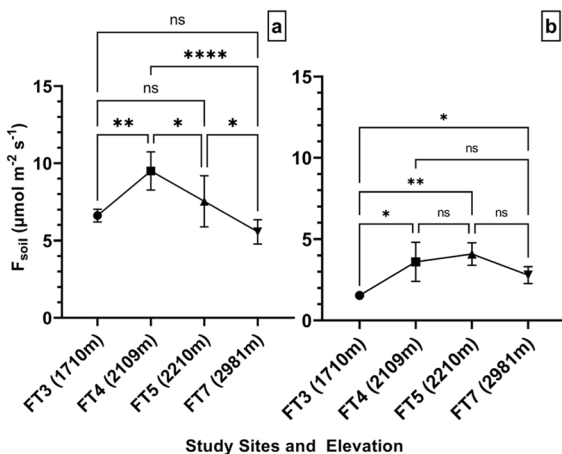


**Fig. 9** Trends in  $F_{soil}$  rates for *Rhododendron arboreum* under different elevations. **a** For the rainy season and **b** for the winter season. Error bars represent standard deviation. \* $p < 0.05$ , \*\* $p < 0.01$ , \*\*\* $p < 0.0001$ , and ns:  $p > 0.05$

## Discussion

### Variation in $F_{soil}$ rates under different forest types

The vegetation composition and density influenced the  $F_{soil}$  rates of the forest types, as indicated by the positive correlation of  $F_{soil}$  with Margalef’s richness index (MR), Shannon–Wiener diversity index ( $H'$ ), and the total biomass density (TBD) (Supplementary Table S7). The selected forest types had different vegetational compositions (Kaushal et al., 2021). The vegetation impacts the  $F_{soil}$  rates through root respiration, soil microclimate, quality, and the quantity of litter input (detritus) (Raich & Tufekciogul, 2000). Hence, we believe the vegetation contributed differentially to these aspects, causing variable  $F_{soil}$  rates under different forest types.

The reduced density and diversity of herbs and shrubs during the winter months, with only a few selective evergreen perennials surviving the harsh cold and drier winters, could explain the positive association of MR and  $H'$  with  $F_{soil}$  in this season. The preponderance of herbaceous vegetation during the rainy season could have masked the impact of tree layer on  $F_{soil}$  rates. Seasonal pattern of herbaceous density is evident in the Himalayas (Joshi et al., 2012; Shameem et al., 2010) and was visually recognizable in the major forest types studied (Fig. 2e, f, h, i, k, and l). So, in addition to the tree species composition and diversity, the forest floor vegetation also impacts the  $F_{soil}$  rates in these major forest types of Central Himalayas on a seasonal basis.

The coniferous- and broadleaf dominant forest types, as well as the tropical, sub-tropical, temperate, sub-alpine, and alpine forest types, did not exhibit any  $F_{soil}$  patterns in common (Fig. 4). Although these trends are prevalent globally (Raich & Tufekciogul, 2000; Yan et al., 2014) and regionally (Joshi, 1994; Kumar et al., 2023; Tewary et al., 1982), the upper temperate to alpine forest types (FT7–FT9) had comparatively lower  $F_{soil}$  rates than the other forest types (Supplementary Table S1). As the forest types are along an elevational gradient (Table 1), they have differential climate and edaphic structures, which could have masked variation due to the forest types. Earlier studies in the region (Joshi et al., 1991; Tewary et al., 1982) were conducted with smaller elevational gradients or a single climate zone, therefore, could elucidate forest-type differences. Given this, Raich and

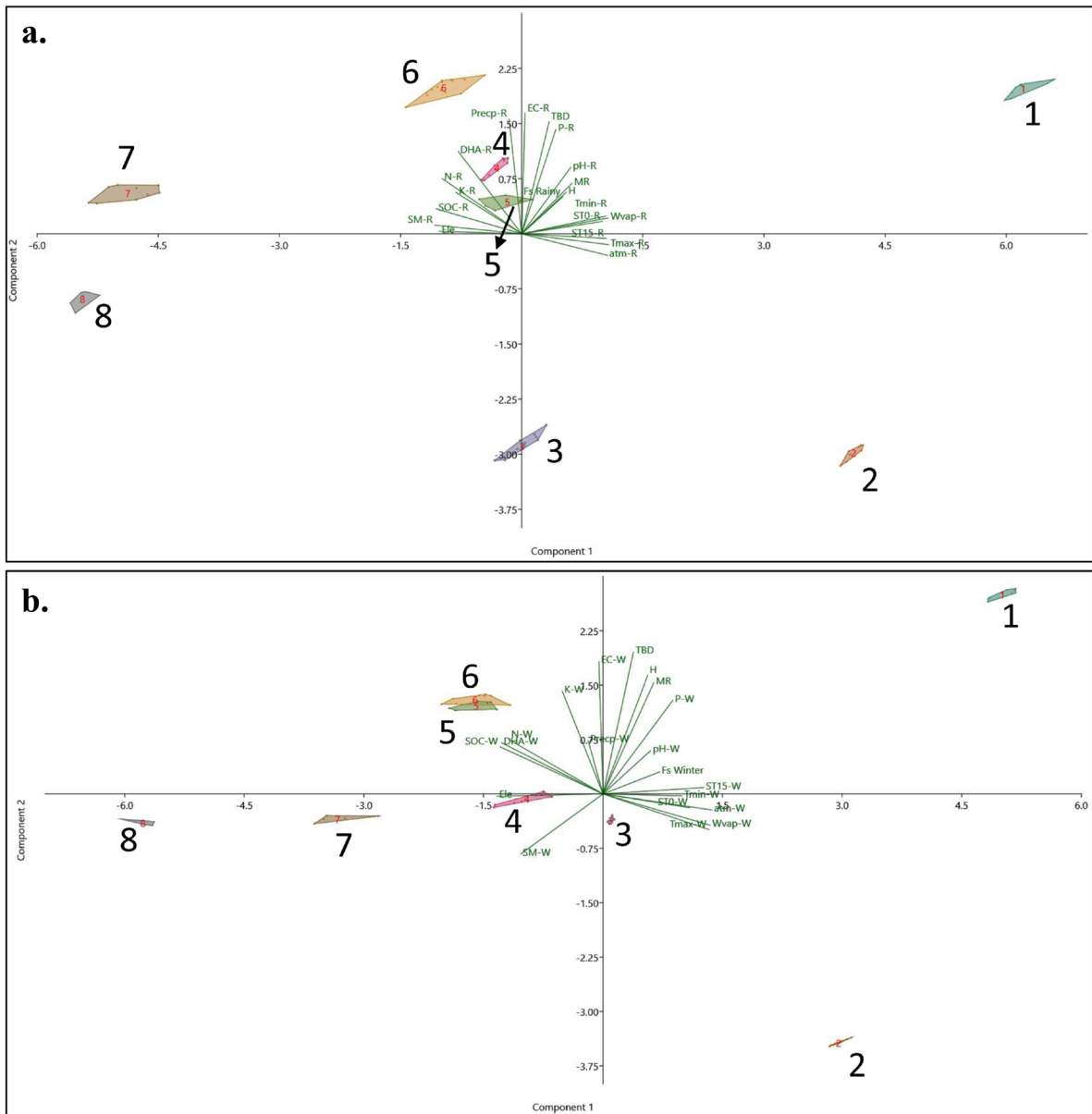


**Fig. 10** PCA biplots indicating PCA scores and loadings for **a** rainy season and **b** winter season. Numerals 1 to 8 represent forest-type PCA score convex hulls

Potter (1995) could also not ascertain the global differential impact of vegetation types on  $F_{\text{soil}}$ .

Temporal variation (seasonal) of  $F_{\text{soil}}$  rates among different forest types and tree species

Despite having higher  $F_{\text{soil}}$  rates during the rainy season, three tree species, viz., *Adina cordifolia* (Roxb.)

Brandis (FT1), *Syzygium cumini* (L.) Skeels (FT1), and *Quercus leucotrichophora* (FT5), did not exhibit significant seasonal variation (Fig. 5) owing to considerable within-season data variance, which masked the between-season variation. Our  $F_{\text{soil}}$  rates were marginally higher than those reported for similar forest types or tree species (Table 2). Interestingly, our results were more comparable to the studies which

used the IRGA-based technique, while those using the alkali-absorption or soda-lime method had noticeably lower values. The IRGA approach is the most sensitive for instantaneous in situ  $F_{\text{soil}}$  measurements and yields higher results than the soda lime method (Pongracic et al., 1997).

The alkali absorption method is known to over or under-estimate the  $F_{\text{soil}}$  rates for spatially heterogeneous environments (King & Harrison, 2002). The IRGA-based systems are sensitive in capturing the seasonal  $F_{\text{soil}}$  variation in forest ecosystems (Ferreira et al., 2018). Thus, a comparison with previous estimates (Table 2) deploying chemical absorption systems would be irrational.

Since the objectives of this study were to capture the variations in  $F_{\text{soil}}$  on account of spatial, temporal, and vegetational features, the use of a chamber-based system was the most appropriate. However, one of the issues of spatial heterogeneity faced by us for the forest-type soil  $\text{CO}_2$  efflux comparisons could be overcome with the eddy covariance technique. Although, a major drawback of this method is that there should be a complete absence of any  $\text{CO}_2$  source or sink element between the soil and eddy flux sensors (Vermue et al., 2008). If this assumption is not met, then the night-time flux estimates will reflect ecosystem level respiration (soil and autotrophic components), as during the daytime, there is a complex interplay of soil respiration, autotrophic respiration, and photosynthesis (Renchon et al., 2021). Regionally, studies incorporating the eddy covariance technique in forest ecosystems used an IRGA-based chamber for determining the rates of soil respiration (Sarma et al., 2022; Singh et al., 2019). In other studies, computing the net ecosystem exchange (NEE) in forest ecosystems determined the total ecosystem respiration and did not represent its constituent elements, i.e., soil respiration and autotrophic respiration (Gnanamoorthy et al., 2020; Rodda et al., 2021). Therefore, for NEE studies, we compared our results only with those which used IRGA-based soil  $\text{CO}_2$  flux chambers for  $F_{\text{soil}}$  determination.

Temperature and soil moisture (regulated through precipitation) are key regulators of the global  $F_{\text{soil}}$  rates (Phillips & Nickerson, 2015; Raich & Potter, 1995; Singh & Gupta, 1977). Microbial activity and organic matter decomposition are positively

influenced by adequate soil temperature and moisture, which increases the heterotrophic component of respiration and, thereby, the  $F_{\text{soil}}$  rates (Singh & Gupta, 1977; Wildung et al., 1975). We found evidence to support this notion in our results wherein under both seasons, soil moisture was positively correlated with soil dehydrogenase enzyme (DHA) activity (Supplementary Fig. S3). The summer and winter seasons had near similar  $F_{\text{soil}}$  rates with the maxima during the rainy season (Fig. 4). Rainy season had 2.8 to 2.2 times greater soil moisture than the summer and winter seasons, respectively. Soil temperature in the rainy season varied insignificantly from the summer, although it had a 2.4 times higher value than the winter. Therefore, maximum  $F_{\text{soil}}$  during the rainy season is due to the elevated soil moisture and warmer temperature. If temperature acted alone, the summer and rainy seasons would have similar  $F_{\text{soil}}$  results.

Rainy season  $F_{\text{soil}}$  maxima could also be due to the increased density of fine root biomass. Regionally, previous studies have established the prominence of fine root biomass and necromass in *Q. leucotrichophora*-, *A. nepalensis*-, and *P. roxburghii*-dominant forest types during the rainy and least during the winter season (Joshi & Garkoti, 2021; Usman et al., 1999). Strong positive statistically significant association between root respiration and fine root biomass is well established globally and regionally (Dilustro et al., 2005; Joshi, 1994; Lee & Jose, 2003). Therefore, the enhanced root biomass and herbaceous growth during the rainy season explain the biotic component behind the rainy season  $F_{\text{soil}}$  maxima.

Other factors associated with the rainy season, such as the prominence of earthworms and soil macrofauna, could also contribute to the higher  $F_{\text{soil}}$  rates (Schulze, 1967). Rainy season  $F_{\text{soil}}$  maxima also indicate that forest types do not suffer from deficient soil  $\text{O}_2$  diffusion due to waterlogging (Davidson et al., 1998). Birch effect (Jarvis et al., 2007) also did not attribute to the  $F_{\text{soil}}$  maxima since the rainy season in the Central Himalayas gradually deposits 65–75% of the total annual rainfall, making it a warm and wet period (Singh & Singh, 1987). Temperature and moisture, combined with several seasonally regulated biotic and abiotic environmental factors, therefore, regulate the temporal variation in the  $F_{\text{soil}}$  rates for these major forest types of Central Himalayas.

**Table 2** A comparative account of  $F_{\text{soil}}$  rates for similar forest types or tree species as our study

Forest type/tree species <sup>Reference</sup>	Location	$F_{\text{soil}}$ rate ( $\mu\text{mol CO}_2 \text{ m}^{-2} \text{ s}^{-1}$ )	Method
Tropical to sub-tropical moist deciduous forests (dipterocarp dominant)			
Mixed dipterocarp forest <sup>e</sup>	China	4–8	c
Dry deciduous forest <sup>g</sup>	Costa Rica	2.35	a
Tropical moist forests <sup>j</sup>	Global	3.33 ± 0.15	d
Tropical deciduous sal mixed forest <sup>f</sup>	Uttar Pradesh, India	5.03 ± 0.45	c
Sub-tropical pine– ( <i>Pinus</i> spp.) dominant forest			
Mixed pine forest <sup>h</sup>	Southeastern, USA	0.78–6.99	c
70-year-old <i>Pinus densiflora</i> forest <sup>i</sup>	Korea	0.13–6.49	c
<i>Pinus kesiya</i> –dominant forest <sup>p</sup>	Meghalaya, India	Around 0.32–1.26	a
Non-degraded pine forest <sup>k</sup>	Uttarakhand, India	1.23–1.20	a
Undisturbed <i>P. roxburghii</i> forest <sup>l</sup>	Uttarakhand, India	1.22–0.24	a
<i>P. roxburghii</i> –dominant forest <sup>m</sup>	Uttarakhand, India	Around 0.32–1.26	a
Deciduous <i>P. roxburghii</i> forest <sup>n</sup>	Uttarakhand, India	12–15	c
95-year-old <i>P. roxburghii</i> plantation forest <sup>o</sup>	Uttarakhand, India	1.09–5.81	c
Moist temperate forest with dominance of Oak ( <i>Quercus</i> spp.)			
Temperate broadleaf ( <i>Quercus lanata</i> and <i>Q. griffithi</i> dominant) <sup>q</sup>	Bhutan	4.2 ± 0.7	c
Upland oak forest <sup>r</sup>	Tennessee, USA	0.8–5.7	c
Oak-hickory forest <sup>s</sup>	Missouri, USA	4.43 ± 1.48	b
<i>Quercus semecarpifolia</i> tree specific <sup>w</sup>	Bhutan	7.9 ± 1.3	c
<i>Q. leucotrichophora</i> –dominant forest <sup>t</sup>	Uttarakhand, India	1.21	a
<i>Q. leucotrichophora</i> mixed forest <sup>u</sup>	Uttarakhand, India	1.58–17.60	c
<i>Q. leucotrichophora</i> – and <i>Q. floribunda</i> –dominant forests <sup>m</sup>	Uttarakhand, India	Around 0.32–2.29	a
<i>Q. leucotrichophora</i> –dominant forest <sup>l</sup>	Uttarakhand, India	0.39–2.27	a
<i>Q. leucotrichophora</i> tree specific <sup>v</sup>	Uttarakhand, India	7.41	c
Moist temperate deciduous forest and temperate coniferous forest			
Temperate coniferous forest <sup>j</sup>	Global	1.80 ± 0.25	d
Temperate deciduous forest <sup>j</sup>	Global	1.71 ± 0.13	d
Old-growth conifer ( <i>Agathis australis</i> ) forest <sup>t</sup>	New Zealand	0.7–9.9	c
<i>R. arboreum</i> forest <sup>x</sup>	Nepal	1.78	c
<i>R. arboreum</i> tree specific <sup>w</sup>	Bhutan	5.6 ± 0.8	c
<i>P. wallichiana</i> –dominant forest <sup>y</sup>	Jammu and Kashmir, India	1.15–4.08	a
<i>C. deodara</i> –dominant forest <sup>m</sup>	Uttarakhand, India	Around 0.32–1.89	a
<i>C. deodara</i> –dominant forest <sup>l</sup>	Uttarakhand, India	0.36–1.78	a
<i>C. deodara</i> –dominant forest <sup>t</sup>	Uttarakhand, India	0.88	a
<i>A. indica</i> tree specific <sup>v</sup>	Uttarakhand, India	25.29	c
<i>R. arboreum</i> tree specific <sup>v</sup>	Uttarakhand, India	8.59	c
<i>C. deodara</i> tree specific <sup>v</sup>	Uttarakhand, India	17.37	c
<i>P. wallichiana</i> tree specific <sup>v</sup>	Uttarakhand, India	15.62	c
Sub-alpine fir forest and alpine scrub			
Alpine Grassland <sup>z</sup>	Swiss Alps	1.7–5.3	c
Tundra <sup>j</sup>	Global	0.16 ± 0.02	d
<i>Abies pindrow</i> –dominant forest <sup>y</sup>	Jammu and Kashmir, India	0.80–2.70	a
Alpine herbaceous meadow <sup>aa</sup>	Uttarakhand, India	3.37 ± 0.21	c



**Table 2** Continued

Forest type/tree species <sup>Reference</sup>	Location	$F_{soil}$ rate ( $\mu\text{mol CO}_2 \text{ m}^{-2} \text{ s}^{-1}$ )	Method
Alpine Sedge meadow <sup>aa</sup>	Uttarakhand, India	2.44 ± 0.12	c
<i>A. pindrow</i> tree specific <sup>v</sup>	Uttarakhand, India	23.11	c

Method: <sup>a</sup>alkali-absorption technique; <sup>b</sup>soda-lime technique; <sup>c</sup>infrared gas analyzer (IRGA)–based chamber method; <sup>d</sup>not specified  
 References: <sup>e</sup>Zhao et al., 2021; <sup>f</sup>Mishra et al., 2020; <sup>g</sup>Schulze, 1967; <sup>h</sup>Dilustro et al., 2005; <sup>i</sup>Noh et al., 2010; <sup>j</sup>Raich and Schlesinger, 1992; <sup>k</sup>Jina et al., 2008; <sup>l</sup>Joshi et al., 1991; <sup>m</sup>Joshi, 1994; <sup>n</sup>Singh et al., 2019; <sup>o</sup>Sivaranjani and Panwar, 2021; <sup>p</sup>Kumar and Ramakrishnan, 1985; <sup>q</sup>Wangdi et al., 2017; <sup>r</sup>Hanson et al., 1993; <sup>s</sup>Ponder, 2005; <sup>t</sup>Tewary et al., 1982; <sup>u</sup>Kumar et al., 2020; <sup>v</sup>Rawat et al., 2021; <sup>w</sup>Nirola, 2016; <sup>x</sup>Dhital et al., 2022; <sup>y</sup>Sundarapandian and Dar, 2013; <sup>z</sup>Grand et al., 2016; <sup>aa</sup>Tiwari et al., 2021

**Impact of surface litter, distance from tree base, and age class of trees on  $F_{soil}$  rates**

We conducted these analyses in the winter season to primarily collect tree-specific (i.e., autotrophic component of soil CO<sub>2</sub> efflux) respiration and minimize the disproportionate impact of the heterotrophic component. During winters, the microbial activity is subdued due to temperature and moisture limitations. Moreover, the roots (autotrophic component) contribute an estimated 50% or more to the total  $F_{soil}$  in Central Himalayas (Joshi, 1994; Joshi et al., 1991; Singh & Gupta, 1977).

Surface litter inclusion only had a positive effect on tropical (FT1) and sub-tropical (FT3) forest types (Supplementary Table S4), with the surface litter making up about 19% of the total  $F_{soil}$  rate (Fig. 6). Our findings were similar to the sub-tropical Himalayan pine forest, where the litter layer contributed 22% to the total soil CO<sub>2</sub> efflux (Joshi et al., 1991). However, the temperate sites (FT4–FT7) had a reverse trend with no contribution (Fig. 6) from surface litter inclusion. Negative surface litter impact was also observed in Central European temperate deciduous forests where low temperature and high precipitation hindered the decomposition activity, thereby reducing litter-based CO<sub>2</sub> efflux (Fekete et al., 2014). Therefore, poor litter decomposition due to subdued microbial activity in the winter season resulted in a negative trend in our temperate elevation forest types. Higher winter temperatures (12–14 °C) in the lower elevations than the temperate sites (4–7 °C) led to greater microbial activity and subsequent surface litter impact. Our findings are consistent with the Central Himalayan pattern, where Singh and Singh (1987) showed that tropical sal forest (like FT1) exhibited faster litter decomposition rates than the sub-tropical

pine forest (like FT3) due to warmer temperatures and intense microarthropod activity.

Even with poor litter respiration, the with-litter  $F_{soil}$  for temperate forests should resemble the without-litter layer and not show lower results comparatively (Fig. 6). We hypothesize that slowly decomposing litter creates an accumulation layer on the soil surface that maintains the soil microclimate, reduces aeration, and serves as a diffusion barrier for soil gases (Walkiewicz et al., 2021). Therefore, removing the litter fraction altered these conditions, increasing the without-litter  $F_{soil}$  rates. The anthropogenic removal of forest floor litter could thus have a detrimental impact in the form of increased  $F_{soil}$  rates in temperate regions. Lower litter respiration in the temperate regions could also be due to smaller measurement time by the IRGA method compared to the 24-h alkali-trap incubation method by the previous studies (Joshi et al., 1991).

For spatial variability (Fig. 7c), only 15% of the tree species investigated showed statistical significance (Supplementary Table S5; Fig. 7). The non-significance for most species was due to larger within-group variation, which masked the variation between the groups (distances from the tree base). Reduction in  $F_{soil}$  rates with increasing distance from the tree base was seen elsewhere, with root biomass as the primary cause for this trend (Lee, 2018; Schwendenmann & Macinnis-Ng, 2016). Globally, the top 40 cm of the soil surface has 75% of the root biomass (Jackson et al., 1996) and up to 90% in the Central Himalayas (Usman et al., 1999). Since our study sites had a significant slope gradient (Table 1), increasing the distance from the tree base might increase the soil surface and horizontal root zone depth, thereby reducing  $F_{soil}$ . Moreover, greater nutrient concentrations caused by stemflow and throughfall (up to 46% in the Himalayas) localize near

the stem base which could have enhanced the  $F_{\text{soil}}$  in this zone (Singh & Singh, 1987).

Only *A. nepalensis*, out of the nine tree species investigated, showed a significant positive linear effect of stem diameter (the corollary of age class) on  $F_{\text{soil}}$  rates (Fig. 8). Different studies have found varying effects of age on  $F_{\text{soil}}$  rates, including positive (Ewel et al., 1987), seasonal (Schurman & Thomas, 2021), and no influence (Wang et al., 2011). The increased root biomass and associated litter inputs, which enhance the autotrophic and heterotrophic components of respiration, are primarily responsible for the positive effect (Bréchet et al., 2011; Ewel et al., 1987; Karki et al., 2021). Since our forest types are natural primary forests with adequate species diversity (Kaushal et al., 2021), we could not capture the spatial variation in  $F_{\text{soil}}$ . The random presence of trees in different girth classes increased the topographic heterogeneity of surrounding vegetation, unlike a plantation with even-aged trees, where the spatial impact is more evident (Ewel et al., 1987). Variable girth classes also impact the edaphic properties and cause microclimatic differences, thereby increasing the background noise and diluting the impact of stem girth on  $F_{\text{soil}}$  rates. The lateral spread of roots and associated  $\text{CO}_2$  efflux for large trees would also not show directly near the base. Further complexities, like the xylary  $\text{CO}_2$  efflux of root respiration from the above-ground parts (Bloemen et al., 2014), reduce the rhizosphere component's impact on  $F_{\text{soil}}$ . Therefore, further research into this aspect is needed to elucidate the driving mechanisms behind the influence of tree size in the Himalayan forests.

Impact of elevation, climatic, and edaphic properties on  $F_{\text{soil}}$  rates along with temperature sensitivity of  $F_{\text{soil}}$

Mean annual maximum and minimum temperature, water vapor pressure, atmospheric pressure, soil temperature, soil moisture, soil organic carbon content, soil Kjeldahl nitrogen, and soil dehydrogenase enzyme activity strongly correlated with elevation (Supplementary figures S3 and S4). Moreover,  $F_{\text{soil}}$  is also strongly correlated with elevation; hence, this creates the situation of multicollinearity among the variables, due to which elevation is subduing the true impact of climatic and edaphic variables on  $F_{\text{soil}}$ . In the event of

multicollinearity, the true relative contribution of the independent variables is difficult to assess (Blalock, 1963). Therefore, comparing our trends with global or regional patterns would be inappropriate.

Smaller vector angles between elevation and soil parameters in the PCA biplot confirm the positive association, and the opposite direction of elevation and climate-associated vectors illustrate their negative association (Fig. 10). Higher elevations being richer in organic carbon, nitrogen, active microbial activity, and soil moisture have reduced  $F_{\text{soil}}$  rates primarily due to lower soil temperature. Similar trends were observed in the Italian Alps, where the  $F_{\text{soil}}$  rates were regulated by temperature (Badrighi et al., 2021). All the forest types were ordinated along PC1 for both seasons in the order of their elevational gradient (Fig. 10). Soil and the atmospheric temperature had one of the highest positive loading correlations with PC1 in both seasons (Supplementary Table S7). Temperature and elevation are, therefore, the chief regulators for  $F_{\text{soil}}$  for major forest types of Central Himalayas along elevational gradients. Soil moisture, edaphic, and other climatic factors also influence  $F_{\text{soil}}$ ; however, temperature is the limiting factor. The alpine regions being rich in soil nutrients, active microbial activity, and soil moisture, should have optimum  $F_{\text{soil}}$ , but are limited by lower soil temperature.

With an increase in elevation, the atmospheric pressure decreases. Moreover, higher elevations being colder result in more condensation and a reduction of water vapor pressure (Korner, 2007). Therefore, high-elevation forest types had lower atmospheric and water vapor pressure than tropical forest types. Greater pressure is associated with reduced  $F_{\text{soil}}$  rates (Davidson et al., 2002; Lund et al., 1999); however, the high atmospheric pressure associated with tropical forests had the highest  $F_{\text{soil}}$  rates while the lowest in the low-pressure alpine region. In our opinion, the impact of temperature and moisture is far greater along the elevation in regulating the  $F_{\text{soil}}$  rates. Therefore, the atmospheric pressure is not causing any significant influence. Moreover, the multicollinearity also hinders the impact in deciphering the associations as discussed earlier. For determining the true impact of climatic constrains such as atmospheric and water vapor pressure within the site, analyses must be conducted modulating the pressure conditions.

We also selected light-associated climatic variables, viz., solar radiation and PAR, since these components

are known to regulate the local microclimate, particularly soil temperature and moisture (Chen et al., 1993), which have been discussed to be critical in influencing the  $F_{\text{soil}}$  rates. Our results corresponded with those of the temperate deciduous forest of the UK where Fenn et al. (2010) found total  $F_{\text{soil}}$  to have no association with solar radiations. Since the studied forest types have medium to high canopy density, other climatic parameters such as temperature were more strongly influencing  $F_{\text{soil}}$ . Being a mountainous region, even the slope aspects also influence the intensity of solar radiations (Singh & Singh, 1987), which could have led to uneven solar radiations influence. Fenn et al. (2010) also attributed the masking influence of soil temperature to the impact of solar radiation on  $F_{\text{soil}}$ . Like solar radiation, PAR did not associate with  $F_{\text{soil}}$  in our study. Although, Mitra et al. (2019) showed PAR as the chief regulator of diurnal variations in  $R_s$  by regulating photosynthesis and rhizosphere activity, however, they reported a 1-to-3-h delay in the response of PAR and  $F_{\text{soil}}$  in their continuous diurnal study. Since our estimates were instantaneous therefore, we did not capture any trend.

Due to its widespread prevalence along the elevational gradient, *R. arboreum* was chosen to study the specie-specific elevation effect on  $F_{\text{soil}}$  rates (Fig. 9). Lower  $F_{\text{soil}}$  rates in the highest and lowest elevations for this species were due to lower soil and atmospheric temperatures in upper temperate FT7 and reduced canopy density in sub-tropical FT3 (Kaushal et al., 2021). Reduced canopy density increases the influx of solar radiations and wind, creating a localized microclimate of increased soil temperature but limiting soil moisture (Badraghi et al., 2021), causing  $F_{\text{soil}}$  reduction.

The absence of any significant association between edaphic properties and  $F_{\text{soil}}$  rates during winter reflects the independence of autotrophic  $R_s$  components towards seasonal soil properties. Maximum  $F_{\text{soil}}$  contribution during winter is due to the autotrophic component (Joshi et al., 1991). Roots also supplement exudates to the microorganisms associated with the rhizosphere region (rhizosphere priming) (Canarini et al., 2019), thereby reducing the impact of bulk soil properties on  $F_{\text{soil}}$ . Among soil properties, for all the forest types, our pH range (4.2–6.8) was above the threshold (pH < 3) to cause pH-associated  $F_{\text{soil}}$  reduction (Luo & Zhou, 2006). The Italian Alps (Badraghi et al., 2021) and the Central Himalayan forests (Joshi,

1994; Joshi et al., 1991; Rawat et al., 2021) showed a positive association of  $F_{\text{soil}}$  with soil pH. The SOC and nitrogen serve as energy and protein sources for the soil microorganisms (Tewary et al., 1982), and positive interaction between these elements and  $F_{\text{soil}}$  is therefore posited (Bargali et al., 1992). However, we obtained a negative correlation due to the multicollinearity of edaphic properties and  $F_{\text{soil}}$  with elevation (Supplementary Fig. S3a). The upper temperate and sub-alpine forest types although having higher concentration of organic carbon and nitrogen show lower  $F_{\text{soil}}$  rates on account of lower temperature which acts as a limiting factor. (Supplementary Fig. S3a). Previous investigations have demonstrated a positive association of soil phosphorous and potassium with  $F_{\text{soil}}$  rates (Bargali et al., 1992). Our study did not observe this association indicating that phosphorous and potassium levels varied along the elevational gradient in these major forest types.

After removing the outliers, the average  $Q_{10}$  for forest types and tree species was approximately 2.30, which aligns with the global median of 2.40 (Raich & Schlesinger, 1992). The  $Q_{10}$  for  $F_{\text{soil}}$  is generally around two as it is a biochemical process (Singh & Gupta, 1977). In our investigation, the  $F_{\text{soil}}$   $Q_{10}$  values for the sub-tropical pine-dominant forest (FT3,  $Q_{10}$  11.80) and the alpine scrub forest (FT9,  $Q_{10}$  9.08) were exorbitantly high. This is primarily due to the reduced vertical forest profile. Alpine meadow (FT9) has no trees or large shrubs; only the prostrate to decumbent shrubs *R. anthopogon* and *Rhododendron lepidotum* Wall. Ex G.Don defines the microclimate (Rai et al., 2012). Sub-tropical FT3 had the lowest stem density among all the sites with tree growth from (sites 1–8) (Kaushal et al., 2021). Therefore, greater daytime solar radiations and surface warming, cooler night-time surface temperatures due to radiative loss (less canopy blanketing), and even stronger wind force (influencing moisture) all lead to larger variations in the temperature and moisture patterns (Rambo & North, 2009). The  $Q_{10}$  also showed a negative correlation (non-significant) with stand density ( $r$ , -0.65). Furthermore, at FT9, the  $Q_{10}$  outside the under-canopy zone of *R. anthopogon* shrubs was 9.08, while that under the shrubs was 4.67. Similarly, the  $Q_{10}$  for pine-dominant (FT3) forest was 11.80, which was higher than *A. nepalensis* ( $Q_{10}$ , 6.11) but nearly identical to *P. roxburghii* ( $Q_{10}$ , 11.94) and *R. arboreum* ( $Q_{10}$ , 12.25). This is because

*A. nepalensis* forms a much denser canopy and dense understory vegetation growth, while *P. roxburghii* has an open sparse canopy, and *R. arboreum* was a scarce understory tree species. Italian Alps (Badraghi et al., 2021) also showed a similar trend where tree height and closeness of canopy modulated the  $Q_{10}$ . Though comparing the  $Q_{10}$  values with global studies seems direct, however, due to the use of different models in the  $Q_{10}$  computation, the comparison of the  $Q_{10}$  values becomes irrational (Fang & Moncrieff, 2001).

## Conclusion

The major forest types chosen demonstrated varying  $F_{\text{soil}}$  rates along the elevational range, which were directly influenced by the species richness and diversity of these forest types. In addition, the stand density of the tree species was also critical since it influences the  $F_{\text{soil}}$  through microclimate regulation. Although no specific pattern existed between the forest types studied, the high-elevation sub-alpine and alpine scrub types had an overall reduced  $F_{\text{soil}}$  rate primarily because of lower soil and atmospheric temperatures. The temporal variation had a uniform impact along the elevational gradient, where the rainy season showed higher  $F_{\text{soil}}$  rates among the forest types and under individual tree species. This trend was primarily regulated by soil moisture and temperature, and neither of these abiotic components alone can lead to higher  $F_{\text{soil}}$  rates. Apart from the abiotic climatic influence, the biotic influence of increased herbaceous/ground vegetation during the rainy season was a probable factor behind this rainy season's  $F_{\text{soil}}$  maxima. The presence of surface litter significantly impacts total  $F_{\text{soil}}$  rates. It enhances the total soil  $\text{CO}_2$  efflux through the contribution from litter decomposition and acts as a barrier layer in cold temperate regions, reducing the overall soil  $\text{CO}_2$  efflux.

Spatially, maximum  $F_{\text{soil}}$  rates were observed near the tree base, which reduces with increasing distance from the base. The age of the trees did not show a clear pattern across the elevational range. Therefore, for tree-associated spatial  $F_{\text{soil}}$  rates further, validation is required. We believe that segregation of the two  $R_s$  components and the corrections for xylary  $\text{CO}_2$  efflux would help decipher the spatial heterogeneity. Soil properties were either negatively

associated or did not show any association with the  $F_{\text{soil}}$  rates. This is primarily because elevation influenced (multicollinearity) soil properties through the abiotic climate variables (temperature and moisture). Very high  $Q_{10}$  values for the alpine scrub and less dense sub-tropical pine forest indicate the temperature sensitivity of these forests. Therefore, these regions will suffer the strongest impact from climate change-associated warming and can be selected as indicators of climate change impact.

Although the forest types are legally present in protected areas, anthropogenic disturbance is evident (Kaushal et al., 2021). Afforestation of forest types having poor stem density is recommended; such an initiative will enhance the biodiversity and carbon stocks, modulate the region's microclimate, and regulate the  $F_{\text{soil}}$  rates. Afforestation plans must preserve the original vegetational composition of the forest types and not alter it significantly. Exotic or commercially important species (e.g., teak, eucalyptus, pine.) must be avoided to prevent a detrimental impact on  $F_{\text{soil}}$  rates. Clearing the forest floor litter for anthropogenic use or through human-induced forest fires is disadvantageous and must be checked. It not only disrupts the nutrient dynamics but also could lead to higher total  $\text{CO}_2$  efflux, as shown by our study. Due to their highest temperature sensitivity, the alpine regions must be stringently monitored for disturbance events such as overgrazing or extraction of alpine shrubs. The conservation of these alpine shrubs is crucial since they are the only major vertical component regulating the microclimate of this region.

Through our research, we were able to identify certain trends and patterns. Subsequent research, particularly which segregates the components of  $F_{\text{soil}}$  and then investigates the impact of vegetation, edaphic, climatic, and other environmental factors, will help to elucidate the mechanisms that control  $F_{\text{soil}}$  in the Himalayas.

**Acknowledgements** The authors express their gratitude to the Principal Chief Conservator of Forests (PCCF) & Chief Wildlife Warden (CWLW), Uttarakhand Forest Department, Uttarakhand, along with the director of Rajaji National Park, and the Divisional Forest Officers (DFOs) for Dehradun, Chakrata, and Kedarnath Wildlife Sanctuary for providing the required field permissions and assistance during the field surveys. We thank Mr. Aakash Goswami for his assistance during the field visits. All authors thank the three anonymous reviewers for their constructive comments and suggestions which considerably improved the manuscript and its readability.

**Author contributions** S. K. and R. B conceptualized this study. S. K. collected the in situ soil CO<sub>2</sub> efflux data and soil sampling, conducted laboratory experiments, performed statistical data analyses and wrote the original manuscript draft. K. S. R., P. L. U., and R. B. reviewed and edited the manuscript. All the authors have read and approved the final version of the manuscript.

**Funding** This study is funded by Science and Engineering Research Board (SERB) through research project no. EEQ/2016/000164. The first author is thankful to the University Grants Commission (UGC), New Delhi, for CSIR-UGC senior research fellowship. The corresponding author acknowledges the Institution of Eminence (IoE), University of Delhi for providing additional funds for the study through Faculty Research Programme (FRP) grant (IoE/2021/12/FRP).

**Data availability** All data generated or analyzed during this study are included in this published article (and its supplementary information files).

**Declarations**

**Ethics approval** Not applicable.

**Consent to participate** Not applicable.

**Consent for publication** Not applicable.

**Competing interests** The authors declare no competing interests.

**References**

Allen, S. E., Grimshaw, H. M., Parkinson, J. A., & Quarmby, C. (1974). *Chemical analysis of ecological materials*. Blackwell Scientific Publications.

Anderson, J. M., & Ingram, J. S. I. (1993). *Tropical soil biology and fertility: A handbook of methods*. C. A. B International, Wallingford, Oxfordshire.

Badraghi, A., Ventura, M., Polo, A., Borruso, L., Giammarchi, F., & Montagnani, L. (2021). Soil respiration variation along an altitudinal gradient in the Italian Alps: Disentangling forest structure and temperature effects. *PLoS ONE*, 16(8), e0247893. <https://doi.org/10.1371/journal.pone.0247893>

Bargali, S. S., Joshi, M., & Bargali, K. (1992). Seasonal pattern of total soil respiration in an age series of Eucalypt plantation and mixed broad-leaved forest in Tarai belt of Kumaun Himalaya. *Oecologia Montana*, 1(2), 7–11.

Bastida, F., Zsolnay, A., Hernández, T., & García, C. (2008). Past, present and future of soil quality indices: A biological perspective. *Geoderma*, 147(3–4), 159–171. <https://doi.org/10.1016/j.geoderma.2008.08.007>

Becker, A., & Bugmann, H. (2001). Global change and mountain regions — An IGBP initiative for collaborative research. In G. Visconti, M. Beniston, & E. D. Iannorelli

(Eds.), *Global change and protected areas. Advances in Global Change Research* (pp. 3–9). Springer, Dordrecht. [https://doi.org/10.1007/0-306-48051-4\\_1](https://doi.org/10.1007/0-306-48051-4_1)

Bhuyan, S. I., Laskar, I., Tripathi, O. P., & Khan, M. L. (2014). Effect of different land use patterns on soil carbon-dioxide emission in Eastern Himalaya. *International Journal of Innovative Science, Engineering and Technology*, 1(9), 476–480.

Blalock, H. M., Jr. (1963). Correlated independent variables: The problem of multicollinearity. *Social Forces*, 42(2), 233–237. <https://doi.org/10.1093/sf/42.2.233>

Bloemen, J., Agneessens, L., Meulebroek, L. V., Aubrey, D. P., McGuire, M. A., Teskey, R. O., & Steppe, K. (2014). Stem girdling affects the quantity of CO<sub>2</sub> transported in xylem as well as CO<sub>2</sub> efflux from soil. *New Phytologist*, 201(3), 897–907. <https://doi.org/10.1111/nph.12568>

Bréchet, L., Ponton, S., Alméras, T., Bonal, D., & Epron, D. (2011). Does spatial distribution of tree size account for spatial variation in soil respiration in a tropical forest? *Plant and Soil*, 347(1), 293–303. <https://doi.org/10.1007/s11104-011-0848-1>

Byanjankar, S., Dhamala, M. K., Maharjan, S. R., & Kayastha, S. P. (2020). Soil respiration and its temperature sensitivity to different ecosystems in Annapurna Conservation Area. *Nepal Journal of Environmental Science*, 8, 69–81. <https://doi.org/10.3126/njes.v8i1.34471>

Canarini, A., Kaiser, C., Merchant, A., Richter, A., & Wanek, W. (2019). Root exudation of primary metabolites: Mechanisms and their roles in plant responses to environmental stimuli. *Frontiers in Plant Science*, 10, 157. <https://doi.org/10.3389/fpls.2019.00157>

Cardoso, E. J. B. N., Vasconcelos, R. L. F., Bini, D., Miyauchi, M. Y. H., Santos, C. A. D., Alves, P. R. L., Paula, A. M. D., Nakatani, A. S., Pereira, J. D. M., & Nogueira, M. A. (2013). Soil health: Looking for suitable indicators. What should be considered to assess the effects of use and management on soil health? *Scientia Agricola*, 70, 274–289. <https://doi.org/10.1590/S0103-90162013000400009>

Casida, L. E., Jr. (1977). Microbial metabolic activity in soil as measured by dehydrogenase determinations. *Applied and Environmental Microbiology*, 34(6), 630–636. <https://doi.org/10.1128/aem.34.6.630-636.1977>

Chakraborty, J. S., Singh, S., Singh, N., & Jeeva, V. (2021). Methane and carbon dioxide flux heterogeneity mediated by termite mounds in moist tropical forest soils of Himalayan foothills, India. *Ecosystems*, 1–16. <https://doi.org/10.1007/s10021-021-00630-y>

Champion, H. G., & Seth, S. K. (1968). *A revised survey of forest types of India*. Natraj Publishers.

Chen, J., Franklin, J. F., & Spies, T. A. (1993). Contrasting microclimates among clearcut, edge, and interior of old-growth Douglas-fir forest. *Agricultural and Forest Meteorology*, 63(3–4), 219–237. [https://doi.org/10.1016/0168-1923\(93\)90061-1](https://doi.org/10.1016/0168-1923(93)90061-1)

Dar, J. A., Ganie, K. A., & Sundarapandian, S. (2015). Soil CO<sub>2</sub> efflux among four coniferous forest types of Kashmir Himalaya. *India. Environmental Monitoring and Assessment*, 187(11), 1–13. <https://doi.org/10.1007/s10661-015-4927-2>

Davidson, E. A., Belk, E., & Boone, R. D. (1998). Soil water content and temperature as independent or confounded factors controlling soil respiration in a temperate mixed

- hardwood forest. *Global Change Biology*, 4(2), 217–227. <https://doi.org/10.1046/j.1365-2486.1998.00128.x>
- Davidson, E. A., Savage, K. V. L. V., Verchot, L. V., & Navarro, R. (2002). Minimizing artifacts and biases in chamber-based measurements of soil respiration. *Agricultural and Forest Meteorology*, 113(1–4), 21–37. [https://doi.org/10.1016/S0168-1923\(02\)00100-4](https://doi.org/10.1016/S0168-1923(02)00100-4)
- Dhital, D., Manandhar, R., Manandhar, P., & Maharjan, S. R. (2022). Soil CO<sub>2</sub> efflux dynamics and its relationship with the environmental variables in a sub-tropical mixed forest. *Open Journal of Forestry*, 12(3), 312–336. <https://doi.org/10.4236/ojf.2022.123017>
- Dilustro, J. J., Collins, B., Duncan, L., & Crawford, C. (2005). Moisture and soil texture effects on soil CO<sub>2</sub> efflux components in southeastern mixed pine forests. *Forest Ecology and Management*, 204(1), 87–97. <https://doi.org/10.1016/j.foreco.2004.09.001>
- Epron, D., Farque, L., Lucot, É., & Badot, P. M. (1999). Soil CO<sub>2</sub> efflux in a beech forest: Dependence on soil temperature and soil water content. *Annals of Forest Science*, 56(3), 221–226. <https://doi.org/10.1051/forest:19990304>
- Ewel, K. C., Cropper Jr, W. P., & Gholz, H. L. (1987). Soil CO<sub>2</sub> evolution in Florida slash pine plantations. I. Changes through time. *Canadian Journal of Forest Research*, 17(4), 325–329. <https://doi.org/10.1139/x87-054>
- Fang, C., & Moncrieff, J. B. (2001). The dependence of soil CO<sub>2</sub> efflux on temperature. *Soil Biology and Biochemistry*, 33(2), 155–165. [https://doi.org/10.1016/S0038-0717\(00\)00125-5](https://doi.org/10.1016/S0038-0717(00)00125-5)
- FAO. (2007). *Digital soil map of the world*. FAO-UN Land and Water Division.
- Fekete, I., Kotroczó, Z., Varga, C., Nagy, P. T., Várbíró, G., Bowden, R. D., Tóth, J. A., & Lajtha, K. (2014). Alterations in forest detritus inputs influence soil carbon concentration and soil respiration in a Central-European deciduous forest. *Soil Biology and Biochemistry*, 74, 106–114. <https://doi.org/10.1016/j.soilbio.2014.03.006>
- Fenn, K. H., Malhi, Y., & Morecroft, M. D. (2010). Soil CO<sub>2</sub> efflux in a temperate deciduous forest: Environmental drivers and component contributions. *Soil Biology & Biochemistry*, 42(10), 1685–1693. <https://doi.org/10.1016/j.soilbio.2010.05.028>
- Ferreira, C. R. P. C., Antonino, A. C. D., Sampaio, E. V. D. S. B., Correia, K. G., Lima, J. R. D. S., Soares, W. D. A., & Menezes, R. S. C. (2018). Soil CO<sub>2</sub> efflux measurements by alkali absorption and infrared gas analyzer in the Brazilian semiarid region. *Revista Brasileira Ciência Do Solo*, 42. <https://doi.org/10.1590/18069657rbcsc20160563>
- Fick, S. E., & Hijmans, R. J. (2017). WorldClim 2: New 1km spatial resolution climate surfaces for global land areas. *International Journal of Climatology*, 37(12), 4302–4315. <https://doi.org/10.1002/joc.5086>
- Friedlingstein, P., O'sullivan, M., Jones, M. W., Andrew, R. M., Hauck, J., Olsen, A., & Zaehele, S. (2020). Global carbon budget 2020. *Earth System Science Data*, 12(4), 3269–3340. <https://doi.org/10.5194/essd-12-3269-2020>
- FSI (2019). *India state of forest report 2019*. Forest Survey of India, Ministry of Environment, Forest and Climate Change. Government of India, Dehradun.
- Giardina, C. P., Litton, C. M., Crow, S. E., & Asner, G. P. (2014). Warming-related increases in soil CO<sub>2</sub> efflux are explained by increased below-ground carbon flux. *Nature Climate Change*, 4, 822–827. <https://doi.org/10.1038/nclimate2322>
- Gnanamoorthy, P., Selvam, V., Burman, P. K. D., Chakraborty, S., Karipot, A., Nagarajan, R., Ramasubramanian, R., Song, Q., Zhang, Y., & Grace, J. (2020). Seasonal variations of net ecosystem (CO<sub>2</sub>) exchange in the Indian tropical mangrove forest of Pichavaram. *Estuarine, Coastal and Shelf Science*, 243, 106828. <https://doi.org/10.1016/j.ecss.2020.106828>
- Grand, S., Rubin, A., Verrecchia, E. P., & Vittoz, P. (2016). Variation in soil respiration across soil and vegetation types in an alpine valley. *PLOS ONE*, 11(9), e0163968. <https://doi.org/10.1371/journal.pone.0163968>
- Hammer, Ø., Harper, D. A. T., & Ryan, P. D. (2001). PAST: Paleontological statistics software package for education and data analysis. *Palaeontologia Electronica*, 4(1), 9.
- Hanson, P. J., Wullschlegel, S. D., Bohlman, S. A., & Todd, D. E. (1993). Seasonal and topographic patterns of forest floor CO<sub>2</sub> efflux from an upland oak forest. *Tree Physiology*, 13(1), 1–15. <https://doi.org/10.1093/treephys/13.1.1>
- Hari, M., & Tyagi, B. (2022). Terrestrial carbon cycle: A tipping edge of climate change between atmosphere and biosphere ecosystems. *Environmental Science: Atmospheres*. <https://doi.org/10.1039/D1EA00102G>
- Jackson, R. B., Canadell, J., Ehleringer, J. R., Mooney, H. A., Sala, O. E., & Schulze, E. D. (1996). A global analysis of root distributions for terrestrial biomes. *Oecologia*, 108(3), 389–411. <https://doi.org/10.1007/BF00333714>
- Jain, A. K. (2020). Geological evolution of the Himalayan mountains. In N. Gupta, S. Tandon (Eds.), *Geodynamics of the Indian Plate* (pp. 363 – 393). Springer Geology, Springer, Cham. [https://doi.org/10.1007/978-3-030-15989-4\\_10](https://doi.org/10.1007/978-3-030-15989-4_10)
- Jarvis, P., Rey, A., Petsikos, C., Wingate, L., Rayment, M., Pereira, J., Banza, J., David, J., Miglietta, F., Borghetti, M., & Manca, G. (2007). Drying and wetting of Mediterranean soils stimulates decomposition and carbon dioxide emission: The “Birch effect.” *Tree Physiology*, 27(7), 929–940. <https://doi.org/10.1093/treephys/27.7.929>
- Jenkins, M. E., & Adams, M. A. (2011). Respiratory quotients and Q<sub>10</sub> of soil respiration in sub-alpine Australia reflect influences of vegetation types. *Soil Biology and Biochemistry*, 43(6), 1266–1274. <https://doi.org/10.1016/j.soilbio.2011.02.017>
- Jina, B. S., Bohra, C. P. S., Rawat, Y. S., & Bhatt, M. D. (2008). Seasonal changes in soil respiration of degraded and non-degraded sites in oak and pine forests of Central Himalaya. *Scientific World*, 6(6), 89–93. <https://doi.org/10.3126/sw.v6i6.2641>
- Joshi, M. (1994). Patterns of forest floor respiration in broad-leaf and conifer forest ecosystems in parts of central Himalaya. *Proceedings of the Indian National Science Academy Part B*, 60, 67–74.
- Joshi, M., Mer, G. S., Singh, S. P., & Rawat, Y. S. (1991). Seasonal pattern of total soil respiration in undisturbed and disturbed ecosystems of Central Himalaya. *Biology and Fertility of Soils*, 11(4), 267–272. <https://doi.org/10.1007/BF00335846>
- Joshi, M., Rawat, Y. S., & Ram, J. (2012). Seasonal variations in species diversity, dry matter and net primary productivity of herb layer of *Quercus leucotrichophora*-*Pinus roxburghii* mixed forest in Kumaun Himalaya. *India*

- Journal of Forestry Research*, 23(2), 223–228. <https://doi.org/10.1007/s11676-011-0214-4>
- Joshi, R. K., & Garkoti, S. C. (2020). Litter dynamics, leaf area index and forest floor respiration as indicators for understanding the role of Nepalese alder in white oak forests in central Himalaya, India. *Ecological Indicators*, 111, 106065. <https://doi.org/10.1016/j.ecolind.2020.106065>
- Joshi, R. K., & Garkoti, S. C. (2021). Influence of Nepalese alder on soil physico-chemical properties and fine root dynamics in white oak forests in the central Himalaya, India. *Catena*, 200, 105140. <https://doi.org/10.1016/j.catena.2020.105140>
- Karhu, K., Auffret, M. D., Dungait, J. A. J., Hopkins, D. W., Prosser, J. I., Singh, B. K., Subke, J. A., Wookey, P. A., Ågren, G. I., Sebasti  , M. T., Gouriveau, F., Bergkvist, G., Meir, P., Nottingham, A. T., Salinas, N., & Hartley, I. P. (2014). Temperature sensitivity of soil respiration rates enhanced by microbial community response. *Nature*, 513(7516), 81–84. <https://doi.org/10.1038/nature13604>
- Karki, H., Bargali, K., & Bargali, S. S. (2021). Spatial and seasonal pattern of fine root biomass and turnover rate in different land use systems in Central Himalaya. *India. Russian Journal of Ecology*, 52(1), 36–48. <https://doi.org/10.1134/S1067413621010070>
- Kaushal, S., & Baishya, R. (2021). Stand structure and species diversity regulate biomass carbon stock under major Central Himalayan forest types of India. *Ecological Processes*, 10, 14. <https://doi.org/10.1186/s13717-021-00283-8>
- Kaushal, S., Siwach, A., & Baishya, R. (2021). Diversity, regeneration, and anthropogenic disturbance in major Indian Central Himalayan forest types: Implications for conservation. *Biodiversity and Conservation*, 30, 2451–2480. <https://doi.org/10.1007/s10531-021-02203-w>
- King, J. A., & Harrison, R. (2002). Measuring soil respiration in the field: An automated closed chamber system compared with portable IRGA and alkali absorption methods. *Communications in Soil Science and Plant Analysis*, 33(3–4), 403–423. <https://doi.org/10.1081/CSS-120002753>
- K  rner, C. (2007). The use of ‘altitude’ in ecological research. *Trends in Ecology & Evolution*, 22(11), 569–574. <https://doi.org/10.1016/j.tree.2007.09.006>
- Kumar, A. D., & Ramakrishnan, P. S. (1985). Litter dynamics in khasi pine (*Pinus kesiya* Royle ex Gordon) of north-eastern India. *Forest Ecology and Management*, 10(1–2), 135–153. [https://doi.org/10.1016/0378-1127\(85\)90018-0](https://doi.org/10.1016/0378-1127(85)90018-0)
- Kumar, P., Singh, R., Singh, H., Chand, T., & Bala, N. (2020). Assessment of soil carbon dioxide efflux and its controlling factors in moist temperate forest of West Himalayas. *Current Science*, 119(4), 661.
- Kumar, S., Kumar, M., Verma, A. K., Joshi, R. K., Hansada, P., Geise, A., & Garkoti, S. K. (2023). Seasonal dynamics of soil and microbial respiration in the banj oak and chir pine forest of the central Himalaya, India. *Applied Soil Ecology*, 182, 104740. <https://doi.org/10.1016/j.apsoil.2022.104740>
- Kuzyakov, Y. (2006). Sources of CO<sub>2</sub> efflux from soil and review of partitioning methods. *Soil Biology and Biochemistry*, 38(3), 425–448. <https://doi.org/10.1016/j.soilbio.2005.08.020>
- Laishram, J., Saxena, K. G., Maikhuri, R. K., & Rao, K. S. (2012). Soil quality and soil health: A review. *International Journal of Ecology and Environmental Sciences*, 38(1), 19–37.
- Lal, R. (2008). Carbon sequestration. *Philosophical Transactions of the Royal Society B: Biological Science*, 363(1492), 815–830
- Lal, R., Monger, C., Nave, L., & Smith, P. (2021). The role of soil in regulation of climate. *Philosophical Transactions of the Royal Society B*, 376(1834), 20210084. <https://doi.org/10.1098/rstb.2021.0084>
- Lashof, D., & Ahuja, D. (1990). Relative contributions of greenhouse gas emissions to global warming. *Nature*, 344, 529–531. <https://doi.org/10.1038/344529a0>
- Lee, J. S. (2018). Relationship of root biomass and soil respiration in a stand of deciduous broadleaved trees—A case study in a maple tree. *Journal of Ecology and Environment*, 42(1), 1–8. <https://doi.org/10.1186/s41610-018-0078-z>
- Lee, K. H., & Jose, S. (2003). Soil respiration, fine root production, and microbial biomass in cottonwood and loblolly pine plantations along a nitrogen fertilization gradient. *Forest Ecology and Management*, 185(3), 263–273. [https://doi.org/10.1016/S0378-1127\(03\)00164-6](https://doi.org/10.1016/S0378-1127(03)00164-6)
- Lei, J., Guo, X., Zeng, Y., Zhou, J., Gao, Q., & Yang, Y. (2021). Temporal changes in global soil respiration since 1987. *Nature Communications*, 12(1), 403. <https://doi.org/10.1038/s41467-020-20616-z>
- Lorenz, K., & Lal, R. (2010). The importance of carbon sequestration in forest ecosystems. In K. Lorenz & R. Lal *Carbon sequestration in forest ecosystems* (1<sup>st</sup> ed., pp. 1 – 21). Springer, Dordrecht. [https://doi.org/10.1007/978-90-481-3266-9\\_6](https://doi.org/10.1007/978-90-481-3266-9_6)
- Lovenduski, N. S., & Bonan, G. B. (2017). Reducing uncertainty in projections of terrestrial carbon uptake. *Environmental Research Letters*, 12(4), 044020. <https://doi.org/10.1088/1748-9326/aa66b8>
- Lund, C. P., Riley, W. J., Pierce, L. L., & Field, C. B. (1999). The effects of chamber pressurization on soil-surface CO<sub>2</sub> flux and the implications for NEE measurements under elevated CO<sub>2</sub>. *Global Change Biology*, 5(3), 269–281.
- Luo, Y., & Zhou, X. (2006). *Soil respiration and the environment*. Academic Press.
- Maier, M., Schack-Kirchner, H., Hildebrand, E. E., & Schindler, D. (2011). Soil CO<sub>2</sub> efflux vs. soil respiration: Implications for flux models. *Agricultural and Forest Meteorology*, 151(12), 1723–1730. <https://doi.org/10.1016/j.agrformet.2011.07.006>
- Mariappan, S., Hartley, I. P., Cressey, E. L., Dungait, J. A., & Quine, T. A. (2022). Soil burial reduces decomposition and offsets erosion-induced soil carbon losses in the Indian Himalaya. *Global Change Biology*, 28(4), 1643–1658. <https://doi.org/10.1111/gcb.15987>
- Metcalfe, D. B., Fisher, R. A., & Wardle, D. A. (2011). Plant communities as drivers of soil respiration: Pathways, mechanisms, and significance for global change. *Biogeosciences*, 8(8), 2047–2061. <https://doi.org/10.5194/bg-8-2047-2011>
- Mishra, S., Chaudhary, L. B., Jain, M. K., Kumar, V., & Behera, S. K. (2020). Interaction of abiotic factor on soil CO<sub>2</sub> efflux in three forest communities in tropical deciduous forest from India. *Environmental Monitoring and Assessment*, 191(Suppl 3), 796. <https://doi.org/10.1007/s10661-019-7689-4>
- Mitra, B., Miao, G., Minick, K., McNulty, S. G., Sun, G., Gavazzi, M., King, J. S., & Noormets, A. (2019).

- Disentangling the effects of temperature, moisture, and substrate availability on soil CO<sub>2</sub> efflux. *Journal of Geophysical Research: Biogeosciences*, 124, 2060–2075. <https://doi.org/10.1029/2019JG005148>
- Mundim, K. C., Baraldi, S., Machado, H. G., & Vieira, F. M. (2020). Temperature coefficient (Q<sub>10</sub>) and its applications in biological systems: Beyond the Arrhenius theory. *Ecological Modelling*, 431, 109127. <https://doi.org/10.1016/j.ecolmodel.2020.109127>
- Nirola, M. P., Wangdi, N., Mayer, M., Schindlbacher, A., & Jandl, R. (2016). Drivers of soil respiration in two mountain forests in Bhutan. *Masters of Science in Mountain Forestry*, University of Natural Resources and Life Sciences.
- Noh, N. J., Son, Y., Lee, S. K., Yoon, T. K., Seo, K. W., Kim, C., Lee, W. K., Bae, S. W., & Hwang, J. (2010). Influence of stand density on soil CO<sub>2</sub> efflux for a *Pinus densiflora* forest in Korea. *Journal of Plant Research*, 123, 411–419. <https://doi.org/10.1007/s10265-010-0331-8>
- Pandey, R., Rawat, M., Singh, R., & Bala, N. (2023). Large scale spatial assessment, modelling and identification of drivers of soil respiration in the Western Himalayan temperate forest. *Ecological Indicators*, 146, 109927. <https://doi.org/10.1016/j.ecolind.2023.109927>
- Phillips, C. L., & Nickerson, N. (2015). Soil respiration. *Reference Module in Earth Systems and Environmental Sciences*, Elsevier. <https://doi.org/10.1016/B978-0-12-409548-9.09442-2>
- Ponder, F., Jr. (2005). Effect of soil compaction and biomass removal on soil CO<sub>2</sub> efflux in a Missouri forest. *Communications in Soil Science and Plant Analysis*, 36(9–10), 1301–1311. <https://doi.org/10.1081/CSS-200056935>
- Pongracic, S., Kirschbaum, M. U. F., & Raison, R. J. (1997). Comparison of soda lime and infrared gas analysis techniques for in situ measurement of forest soil respiration. *Canadian Journal of Forest Research*, 27(11), 1890–1895. <https://doi.org/10.1139/x97-139>
- Rai, I. D., Adhikari, B. S., & Rawat, G. S. (2012). Floral diversity along sub-alpine and alpine ecosystems in Tungnath area of Kedarnath Wildlife Sanctuary. *Uttarakhand Indian Forester*, 138(10), 927.
- Raich, J. W., & Potter, C. S. (1995). Global patterns of carbon dioxide emissions from soils. *Global Biogeochemical Cycles*, 9(1), 23–36. <https://doi.org/10.1029/94GB02723>
- Raich, J. W., & Schlesinger, W. H. (1992). The global carbon dioxide flux in soil respiration and its relationship to vegetation and climate. *Tellus b: Chemical and Physical Meteorology*, 44(2), 81–99. <https://doi.org/10.3402/tellusb.v44i2.15428>
- Raich, J. W., & Tufekciogul, A. (2000). Vegetation and soil respiration: Correlations and controls. *Biogeochemistry*, 48(1), 71–90. <https://doi.org/10.1023/A:100612000616>
- Rambo, T. R., & North, M. P. (2009). Canopy microclimate response to pattern and density of thinning in a Sierra Nevada forest. *Forest Ecology and Management*, 257(2), 435–442. <https://doi.org/10.1016/j.foreco.2008.09.029>
- Ramesh, S., Manjiaiah, K. M., Tomar, J. M. S., & Ngachan, S. V. (2013). Effect of multipurpose tree species on soil fertility and CO<sub>2</sub> efflux under hilly ecosystems of Northeast India. *Agroforestry Systems*, 87(6), 1377–1388. <https://doi.org/10.1007/s10457-013-9645-6>
- Rawat, M., Arunachalam, K., & Arunachalam, A. (2021). Tree species influence soil respiration in a temperate forest of Uttarakhand Himalaya. *India. Journal of Sustainable Forestry*, 40(8), 820–830. <https://doi.org/10.1080/10549811.2020.1822873>
- Renchon, A. A., Drake, J. E., Macdonald, C. A., Sihi, D., Hinko-Najera, N., Tjoelker, M. G., & Pendall, E. (2021). Concurrent measurements of soil and ecosystem respiration in a mature eucalypt woodland: advantages, lessons, and questions. *Journal of Geophysical Research: Biogeosciences*, 126(3), e2020JG006221. <https://doi.org/10.1029/2020JG006221>
- Rodda, S. R., Thumaty, K. C., Praveen, M. S. S., Jha, C. S., & Dadhwal, V. K. (2021). Multi-year eddy covariance measurements of net ecosystem exchange in tropical dry deciduous forest of India. *Agricultural and Forest Meteorology*, 301, 108351. <https://doi.org/10.1016/j.agrformet.2021.108351>
- Sánchez-Cañete, E. P., Barron-Gafford, G. A., & Chorover, J. (2018). A considerable fraction of soil-respired CO<sub>2</sub> is not emitted directly to the atmosphere. *Scientific Reports*, 8(1), 1–10. <https://doi.org/10.1038/s41598-018-29803-x>
- Sanders, N. J., & Rahbek, C. (2012). The patterns and causes of elevational diversity gradients. *Ecography*, 35(1), 1–3. <https://doi.org/10.1111/j.1600-0587.2011.07338.x>
- Sarma, D., Burman, P. K. D., Chakraborty, S., Gogoi, N., Bora, A., Metya, A., Datye, A., Murkute, C., & Karipot, A. (2022). Quantifying the net ecosystem exchange at a semi-deciduous forest in northeast India from intra-seasonal to the seasonal time scale. *Agricultural and Forest Meteorology*, 314, 108786. <https://doi.org/10.1016/j.agrformet.2021.108786>
- Schickhoff, U., Singh, R. B., & Mal, S. (2016). Climate change and dynamics of glaciers and vegetation in the Himalaya: An overview. In R. Singh, U. Schickhoff, & S. Mal (Eds.), *Climate change, glacier response, and vegetation dynamics in the Himalaya* (1st ed., pp. 1–26). Springer, Cham. [https://doi.org/10.1007/978-3-319-28977-9\\_1](https://doi.org/10.1007/978-3-319-28977-9_1)
- Schulze, E. D. (1967). Soil respiration of tropical vegetation types. *Ecology*, 48(4), 652–653. <https://doi.org/10.2307/1936509>
- Schurman, J. S., & Thomas, S. C. (2021). Linking soil CO<sub>2</sub> efflux to individual trees: Size-dependent variation and the importance of the Birch effect. *Soil Systems*, 5(1), 7. <https://doi.org/10.3390/soilsystems5010007>
- Schwendenmann, L., & Macinnis-Ng, C. (2016). Soil CO<sub>2</sub> efflux in an old-growth southern conifer forest (*Agathis australis*)—magnitude, components and controls. *The Soil*, 2(3), 403–419. <https://doi.org/10.5194/soil-2-403-2016>
- Shameem, S. A., Soni, P., & Bhat, G. A. (2010). Comparative study of herb layer diversity in lower Dachigam National Park, Kashmir Himalaya, India. *International Journal of Biodiversity and Conservation*, 2(10), 308–315.
- Singh, D., Sharma, P., Kumar, U., Daverey, A., & Arunachalam, K. (2021). Effect of forest fire on soil microbial biomass and enzymatic activity in oak and pine forests of Uttarakhand Himalaya. *India. Ecological Processes*, 10(1), 29. <https://doi.org/10.1186/s13717-021-00293-6>
- Singh, J. S., & Gupta, S. R. (1977). Plant decomposition and soil respiration in terrestrial ecosystems. *The Botanical Review*, 43(4), 449–528. <https://doi.org/10.1007/BF02860844>
- Singh, J. S., & Singh, S. P. (1987). Forest vegetation of the Himalaya. *The Botanical Review*, 53(1), 80–192. <https://doi.org/10.1007/BF02858183>



- Singh, N., & Parida, B. R. (2019). Environmental factors associated with seasonal variations of night-time plant canopy and soil respiration fluxes in deciduous conifer forest, Western Himalaya. *India. Trees*, 33(2), 599–613. <https://doi.org/10.1007/s00468-018-1804-y>
- Singh, N., Parida, B. R., Charakborty, J. S., & Patel, N. R. (2019). Net ecosystem exchange of CO<sub>2</sub> in deciduous pine forest of lower Western Himalaya. *India. Resources*, 8(2), 98. <https://doi.org/10.3390/resources8020098>
- Sivaranjani, S., & Panwar, V. P. (2021). Environmental controls and influences of *Pinus roxburghii* Sarg. (Chir pine) plantation on temporal variation in soil carbon dioxide emission and soil organic carbon stock under humid subtropical region. *Environmental Monitoring and Assessment*, 193, 1–14. <https://doi.org/10.1007/s10661-021-09419-x>
- Sundarapandian, S., & Dar, J. (2013). Variation in soil CO<sub>2</sub> efflux in *Pinus wallichiana* and *Abies pindrow* temperate forests of Western Himalayas. *India. Forest Research*, 3(116), 2. <https://doi.org/10.4172/2168-9776.1000116>
- Tewary, C. K., Pandey, U., & Singh, J. S. (1982). Soil and litter respiration rates in different microhabitats of a mixed oak-conifer forest and their control by edaphic conditions and substrate quality. *Plant and Soil*, 65(2), 233–238. <https://doi.org/10.1007/BF02374653>
- Tiwari, P., Bhattacharya, P., Rawat, G. S., Rai, I. D., & Talukdar, G. (2021). Experimental warming increases ecosystem respiration by increasing above-ground respiration in alpine meadows of Western Himalaya. *Scientific Reports*, 11(1), 2640. <https://doi.org/10.1038/s41598-021-82065-y>
- Trumbore, S. (2006). Carbon respired by terrestrial ecosystems—recent progress and challenges. *Global Change Biology*, 12(2), 141–153. <https://doi.org/10.1111/j.1365-2486.2006.01067.x>
- Usman, S., Singh, S. P., & Rawat, Y. S. (1999). Fine root productivity and turnover in two evergreen central Himalayan forests. *Annals of Botany*, 84(1), 87–94. <https://doi.org/10.1006/anbo.1999.0894>
- Vermue, E., Elbers, J., & Hoosbeek, M. (2008). A comparative field study of four soil respiration systems. Accessed on 18 March 2023 <https://edepot.wur.nl/120659>
- Vikram, K., Chaudhary, H., Notup, T., Dinakaran, J., & Rao, K. S. (2022). Soil respiration under different land use systems in Kumaon region of Central Himalaya, India. *International Journal of Ecology and Environmental Sciences*, 48(5), 649–661. <https://doi.org/10.55863/ijees.2022.0649>
- Walkiewicz, A., Rafalska, A., Bulak, P., Bieganski, A., & Osborne, B. (2021). How can litter modify the fluxes of CO<sub>2</sub> and CH<sub>4</sub> from forest soils? *A Mini-Review. Forests*, 12(9), 1276. <https://doi.org/10.3390/f12091276>
- Wang, B., Jiang, Y., Wei, X., Zhao, G., Guo, H., & Bai, X. (2011). Effects of forest type, stand age, and altitude on soil respiration in subtropical forests of China. *Scandinavian Journal of Forest Research*, 26(1), 40–47. <https://doi.org/10.1080/02827581.2010.538082>
- Wangdi, N., Mayer, M., Nirola, M. P., Zangmo, N., Orong, K., Ahmed, I. U., Darabant, A., Jandl, R., Gratzner, G., & Schindlbacher, A. (2017). Soil CO<sub>2</sub> efflux from two mountain forests in the eastern Himalayas, Bhutan: Components and controls. *Biogeosciences*, 14(1), 99–110. <https://doi.org/10.5194/bg-14-99-2017>
- Wani, O. A., Kumar, S., Hussain, N., Wani, A. I. A., Subhash, B., Parvej, A., Rashid, M., Popescu, S. M., & Mansoor, S. (2022). Multi-scale processes influencing global carbon storage and land-carbon-climate nexus: A critical review. *Pedosphere*. <https://doi.org/10.1016/j.pedsph.2022.07.002>
- Wildung, R. E., Garland, T. R., & Buschbom, R. L. (1975). The interdependent effects of soil temperature and water content on soil respiration rate and plant root decomposition in arid grassland soils. *Soil Biology and Biochemistry*, 7(6), 373–378. [https://doi.org/10.1016/0038-0717\(75\)90052-8](https://doi.org/10.1016/0038-0717(75)90052-8)
- Yan, W. D., Xu, W. M., Tian, D. L., Peng, Y. Y., Zhen, W., Zhang, C., & Xu, J. (2014). Soil CO<sub>2</sub> flux in different types of forests under a subtropical microclimatic environment. *Pedosphere*, 24(2), 243–250. [https://doi.org/10.1016/S1002-0160\(14\)60010-2](https://doi.org/10.1016/S1002-0160(14)60010-2)
- Zhao, J. F., Liao, Z. Y., Yang, L. Y., Shi, J. K., & Tan, Z. H. (2021). Characteristics of soil respiration and its components of a mixed dipterocarp forest in China. *Forests*, 12(9), 1159. <https://doi.org/10.3390/f12091159>
- Zuur, A. F., Ieno, E. N., & Smith, G. M. (2007). *Analysing ecological data*. Springer.

**Publisher's Note** Springer Nature remains neutral with regard to jurisdictional claims in published maps and institutional affiliations.

Springer Nature or its licensor (e.g. a society or other partner) holds exclusive rights to this article under a publishing agreement with the author(s) or other rightsholder(s); author self-archiving of the accepted manuscript version of this article is solely governed by the terms of such publishing agreement and applicable law.